

Far field operator splitting and completion in inverse medium scattering

Roland Griesmaier*  and Lisa Schätzle* 

Institut für Angewandte und Numerische Mathematik, Karlsruher Institut für Technologie, Englerstr. 2, 76131 Karlsruhe, Germany

E-mail: roland.griesmaier@kit.edu and lisa.schaetzle@kit.edu

Received 10 January 2024; revised 15 August 2024

Accepted for publication 18 September 2024

Published 8 October 2024



CrossMark

Abstract

We study scattering of time-harmonic plane waves by compactly supported inhomogeneous objects in a homogeneous background medium. The far field operator associated to a fixed scatterer describes multi-static remote observations of scattered fields corresponding to arbitrary superpositions of plane wave incident fields at a single frequency. In this work we consider far field operators for systems of two well-separated scattering objects, and we discuss the non-linear inverse problem to recover the far field operators associated to each of these two scatterers individually. This is closely related to the question whether the two components of the scatterer can be distinguished by means of inverse medium scattering in a stable way. We also study the restoration of missing or inaccurate components of an observed far field operator and comment on the benefits of far field operator splitting in this context. Both problems are ill-posed without further assumptions, but we give sufficient conditions on the diameter of the supports of the scatterers, the distance between them, and the size of the missing or corrupted data component to guarantee stable recovery whenever sufficient *a priori* information on the location of the unknown scatterers is available. We provide algorithms, error estimates, a stability analysis, and we demonstrate our theoretical predictions by numerical examples.

Keywords: inverse medium scattering, Helmholtz equation, far field operator splitting, data completion

* Authors to whom any correspondence should be addressed.



Original Content from this work may be used under the terms of the [Creative Commons Attribution 4.0 licence](https://creativecommons.org/licenses/by/4.0/). Any further distribution of this work must maintain attribution to the author(s) and the title of the work, journal citation and DOI.

1. Introduction

The inverse medium scattering problem (see, e.g. [14, p 439]) is to determine the shape and the refractive index of a compactly supported inhomogeneous object from a knowledge of the far field patterns of scattered waves corresponding to plane wave incident fields for all possible illumination and observation directions on the unit sphere. These input data can be described by the far field operator, which maps densities of superpositions of plane wave incident fields to the far field patterns of the corresponding scattered fields. The far field operator can be viewed as an idealized measurement operator for the inverse medium scattering problem, and accordingly it plays a central role in several reconstruction methods (see, e.g. [1, 11, 12, 15, 26, 35] and the monographs [9, 10, 14, 38]). In this work we do not investigate the inverse scattering problem itself, but we focus on two related inverse problems. To this end we restrict the discussion to the two-dimensional case and consider scatterers that consist of two well-separated components. Assuming that a possibly noisy and incomplete version of the associated far field operator is available, we ask the following questions:

- (a) Is it possible to reconstruct the far field operators associated to the two components of the scatterer individually, if we have some *a priori* information on the location of these components?
- (b) Can we recover missing parts of the far field operator and filter possible data errors, and why can far field operator splitting be useful in this context?

Regarding problem (a), the uniqueness of solutions to the inverse medium scattering problem (see [8, 42, 44, 46]) tells us that the shape and the refractive index of the scattering object are uniquely determined by the far field operator. Accordingly, having some *a priori* information about the location of the two components of the scattering object, one could first reconstruct the scatterer, then split it into its two components, and finally calculate the far field operators corresponding to these two components for solving problem (a). However, solving the inverse medium scattering problem is time-consuming and severely ill-posed, and we will show that it is actually not required for solving problem (a). Similarly, it is well-known that the far field pattern depends analytically on both the illumination and the observation direction (see, e.g. [14, 27]). Thus recovering missing parts of the far field operator in problem (b) is usually possible, if the available data patch is not too small, but also severely ill-posed without further assumptions.

For both questions we will assume that we have access to an estimate of the location and possibly the size of the (two components of) the unknown scatterer, and our goal is to solve the inverse problems (a) and (b) without solving the inverse medium scattering problem itself. The *a priori* information on the location of the (two components of the) scatterer is used to develop sparse decompositions of the associated far field operators with respect to suitably modulated Fourier representations of the Hilbert–Schmidt kernels of these operators. These sparse representations are the foundation of our reconstruction methods. Apart from that the main theoretical contributions of this work are error estimates and a rigorous stability analysis for our reconstruction algorithms. These results build on previous investigations of far field splitting and data completion for the inverse source problem in [25, 28–31]. There are two main differences distinguishing the inverse source problem considered in these works and the inverse medium scattering problem considered here. The first difference is that, while for the inverse source problem one has access to just one far field pattern radiated by the unknown source, infinitely many but correlated far field patterns corresponding to plane wave incident fields for all possible illumination directions are available for the inverse medium scattering

problem. We will show that, by working with whole far field operators instead of individual far field patterns, correlations in this data set beyond simple reciprocity relations can be used to obtain better stability estimates for reconstruction methods for problems (a) and (b) for the inverse medium scattering problem, when compared to the corresponding stability estimates for the inverse source problem in [25, 29]. The second difference is that the far field splitting problem for inverse source problems is linear, while it is nonlinear for the inverse medium scattering problem due to multiple scattering effects. To untangle multiple scattering we decompose far field operators corresponding to systems of two scatterers using the Born series and consider sparse representations of the various parts in this decomposition. These can then be distinguished by our splitting algorithm.

The (inverse) Born series has recently also been used directly in reconstruction methods for the inverse medium scattering problem in [17, 33, 34]. In [6] (see also [21, 22]) the authors apply a reduced order model to transform scattering data for a time-dependent scattering problem including multiple scattering effects to observations expected in the Born approximation, i.e. multiple scattering effects are removed. Both approaches are not directly related to the results in this work. We also note that alternate methods for far field splitting for inverse source problems have been proposed in [5, 45], and that splitting problems for time-dependent waves have more recently been considered in [3, 24, 32]. Data completion for far field operators as in problem (b) has recently also been discussed in [20, 41] (see also [2, 7] for related results for the Cauchy problem for the Helmholtz equation). In contrast to our work, these authors do not use sparse representations of far field patterns or far field operators with respect to modulated Fourier bases to stabilize their algorithms, which so far also lack a rigorous stability analysis.

Being able to split and complete far field operators has important implications for the inverse medium scattering problem. If one can stably split the far field operator corresponding to a system of two scatterers, then these scatterers can also be distinguished in the reconstruction, which tells something about resolution in the presence of noise. On the other hand incomplete data sets are common in applications, while reconstruction methods usually work more stably for complete data sets. Being able to reliably restore the full far field operator helps to reduce the effect of this additional source of ill-posedness.

The outline of this paper is as follows. After providing some theoretical background on inverse medium scattering, we develop sparse representations of far field operators based on the Born series and modulated Fourier expansions in section 2. In section 3 we pursue far field operator splitting, first using the Born approximation and neglecting multiple scattering, and later including multiple scattering effects. Far field operator completion is the topic of section 4. In section 5 we provide numerical examples to illustrate our theoretical findings, and we close with some concluding remarks.

2. Inhomogeneous medium scattering

We consider time-harmonic wave propagation in the plane. Let $D \subseteq \mathbb{R}^2$ be bounded such that the boundary ∂D of D is of Lipschitz class. Suppose that $n^2 = 1 + q$ represents the *index of refraction*, where the real-valued *contrast function* $q \in L^\infty(D)$ satisfies $q > -1$ in D and is extended by $q = 0$ outside D .

Let $k > 0$ be the wave number, and let

$$u^i(x; d) := e^{ikx \cdot d}, \quad x \in \mathbb{R}^2, \quad (2.1a)$$

be an incident plane wave with illumination direction $d \in S^1$. The scattering problem is then to determine the *total field* $u_q \in H_{\text{loc}}^1(\mathbb{R}^2)$ with

$$\Delta u_q + k^2 n^2 u_q = 0 \quad \text{in } \mathbb{R}^2, \quad (2.1b)$$

such that the *scattered field* $u_q^s = u_q - u^i$ satisfies the *Sommerfeld radiation condition*

$$\lim_{r \rightarrow \infty} \sqrt{r} \left(\frac{\partial u_q^s}{\partial r}(x; d) - i k u_q^s(x; d) \right) = 0, \quad r = |x|, \quad (2.1c)$$

uniformly with respect to all directions $x/|x| \in S^1$. As for the incident field, we indicate the dependence of the total and scattered fields on the illumination direction by a second argument.

Remark 2.1. The Helmholtz equation (2.1b) has to be understood in the weak sense, i.e. $u_q \in H_{\text{loc}}^1(\mathbb{R}^2)$ is a solution if and only if

$$\int_{\mathbb{R}^2} (\nabla u_q \cdot \nabla v - k^2 n^2 u_q v) \, dx = 0 \quad \text{for all } v \in C_0^\infty(\mathbb{R}^2).$$

Standard regularity results yield smoothness of u_q and u_q^s in $\mathbb{R}^2 \setminus \overline{B_R(0)}$, where $B_R(0)$ is a sufficiently large ball containing the scatterer D . \diamond

The scattering problem (2.1) has a unique solution $u_q \in H_{\text{loc}}^1(\mathbb{R}^2)$ (see, e.g. [37, theorem 7.13]). This solution satisfies the *Lippmann–Schwinger integral equation*

$$u_q(x; d) = u^i(x; d) + k^2 \int_{\mathbb{R}^2} q(y) \Phi(x-y) u_q(y; d) \, dy, \quad x \in D, \quad (2.2)$$

where $\Phi(x) := i/4 H_0^{(1)}(k|x|)$, $x \neq 0$, denotes the *fundamental solution* to the Helmholtz equation (see e.g. [37, theorem 7.12]). In fact, this integral equation is uniquely solvable in $L^2(D)$, and its solution can be extended by the right hand side of (2.2) to a solution of the scattering problem (2.1) (see, e.g. [37, theorem 7.12]). The scattered field satisfies the *far field expansion*

$$u_q^s(x; d) = \frac{e^{i\pi/4}}{\sqrt{8\pi}} \frac{e^{ik|x|}}{\sqrt{k|x|}} u_q^\infty(\hat{x}; d) + O(|x|^{-3/2}), \quad |x| \rightarrow \infty,$$

uniformly in all directions $\hat{x} := x/|x| \in S^1$. The *far field pattern* $u_q^\infty \in L^2(S^1)$ is given by

$$u_q^\infty(\hat{x}; d) = k^2 \int_D q(y) u_q(y; d) e^{-ik\hat{x} \cdot y} \, dy, \quad \hat{x} \in S^1,$$

(see, e.g. [37, theorem 7.15]). It satisfies the *reciprocity relation*

$$u_q^\infty(\hat{x}; d) = u_q^\infty(-d; -\hat{x}), \quad \hat{x}, d \in S^1, \quad (2.3)$$

(see [14, theorem 8.8]). The far field patterns $u_q^\infty(\hat{x}; d)$ for all $\hat{x}, d \in S^1$ define the *far field operator*

$$F_q : L^2(S^1) \rightarrow L^2(S^1), \quad (F_q g)(\hat{x}) := \int_{S^1} u_q^\infty(\hat{x}; d) g(d) \, ds(d), \quad (2.4)$$

which maps densities of arbitrary superpositions of incident plane waves to the far field patterns of the corresponding scattered fields. The far field operator is compact and normal (see, e.g. [37, theorem 7.20]), and it is a trace class operator (see [13]). In particular, $F_q \in \text{HS}(L^2(S^1))$, where $\text{HS}(L^2(S^1))$ denotes the space of compact linear operators $A : L^2(S^1) \rightarrow L^2(S^1)$ with $\text{tr}(A^*A) < \infty$, i.e. the space of Hilbert–Schmidt operators on $L^2(S^1)$ (see, e.g. [47, p 210]).

2.1. Two inverse problems

In this work we are interested in the following two inverse problems.

- (a) **Far field operator splitting:** suppose that $D = D_1 \cup D_2$ for some well-separated bounded Lipschitz domains $D_1, D_2 \subseteq \mathbb{R}^2$, i.e. we assume that there exist balls $B_{R_j}(c_j), j = 1, 2$, with $D_j \subseteq B_{R_j}(c_j)$ and $|c_1 - c_2| > R_1 + R_2$. Accordingly, let $q_1 := q|_{D_1}$ and $q_2 := q|_{D_2}$ denote the contrast functions of the two components of the scatterer. The goal of *far field operator splitting* is then to recover the far field operators F_{q_1} and F_{q_2} corresponding to the two components of the scatterer from F_q . Since $q = q_1 + q_2$ is uniquely determined by F_q (see [8, 42, 44, 46]), this inverse problem is uniquely solvable, whenever sufficient a priori information on the locations of the scatterers D_1 and D_2 is available to determine q_1 and q_2 from q . In this work we will assume that balls $B_{R_1}(c_1)$ and $B_{R_2}(c_2)$ as above containing the scatterers are known a priori, and we use this information to develop stability estimates and reconstruction algorithms.
- (b) **Far field operator completion:** suppose that the far field pattern $u_q^\infty(\hat{x}; d)$ cannot be observed for all illumination directions $d \in S^1$ and for all observation directions $\hat{x} \in S^1$ but only observations of $u_q^\infty(\hat{x}; d)$ for $(\hat{x}, d) \in \Omega^c := (S^1 \times S^1) \setminus \Omega$ for some $\Omega \subseteq S^1 \times S^1$ are available. Accordingly, we define the *restricted far field operator*

$$F_q|_{\Omega^c} : L^2(S^1) \rightarrow L^2(S^1), (F_q|_{\Omega^c} g)(\hat{x}) := \int_{S^1} \chi_{\Omega^c}(\hat{x}, d) u_q^\infty(\hat{x}; d) g(d) ds(d). \quad (2.5)$$

The goal of *far field operator completion* is then to recover F_q from $F_q|_{\Omega^c}$. Since the far field pattern is a real analytic function on $S^1 \times S^1$ (see, e.g. [14, 27]), this inverse problem has a unique solution as long as Ω^c has an interior point. We will assume that a ball $B_R(c)$ with $D \subseteq B_R(c)$ is known a priori, and we use this information to develop stability estimates and reconstruction algorithms.

2.2. Far field translation

Translating the scatterer by $c \in \mathbb{R}^2$ changes the incident field at the location of the scatterer and thus also the scattered field as well as its far field pattern. Considering the shifted contrast function

$$q_c(x) := q(x + c), \quad x \in \mathbb{R}^2, \quad (2.6)$$

the associated far field pattern is given by

$$u_{q_c}^\infty(\hat{x}; d) = e^{-ikc \cdot (d - \hat{x})} u_q^\infty(\hat{x}; d), \quad \hat{x} \in S^1,$$

and the far field operator satisfies, for $g \in L^2(S^1)$,

$$(F_{q_c} g)(\hat{x}) = e^{ikc \cdot \hat{x}} \int_{S^1} e^{-ikc \cdot d} g(d) u_q^\infty(\hat{x}; d) ds(d), \quad \hat{x} \in S^1.$$

Introducing

$$T_c : L^2(S^1) \rightarrow L^2(S^1), \quad (T_c g)(\hat{x}) := e^{ikc\hat{x}} g(\hat{x}), \quad (2.7)$$

and

$$\mathcal{T}_c : \text{HS}(L^2(S^1)) \rightarrow \text{HS}(L^2(S^1)), \quad \mathcal{T}_c G := T_c \circ G \circ T_{-c}, \quad (2.8)$$

where $G : L^2(S^1) \rightarrow L^2(S^1)$ is a Hilbert–Schmidt operator, we have $F_{q_c} = \mathcal{T}_c F_q$. We call \mathcal{T}_c the *translation operator*.

Lemma 2.2. *Let $c \in \mathbb{R}^2$. The operator $\mathcal{T}_c \in \mathcal{L}(\text{HS}(L^2(S^1)))$ is unitary with $\mathcal{T}_c^* = \mathcal{T}_{-c}$.*

Proof. The adjoint of T_c from (2.7) is given by $T_c^* = T_{-c}$, and (2.8) implies that, for any $G, H \in \text{HS}(L^2(S^1))$,

$$\langle \mathcal{T}_c G, H \rangle_{\text{HS}} = \text{tr}((T_c G T_{-c})^* H) = \text{tr}(T_{-c} H T_c G^*) = \text{tr}(G^* T_{-c} H T_c) = \langle G, \mathcal{T}_{-c} H \rangle_{\text{HS}}.$$

This shows that $\mathcal{T}_c^* = \mathcal{T}_{-c}$, which is the same as \mathcal{T}_c^{-1} . \square

2.3. The Born series

For any $d \in S^1$ the Lippmann–Schwinger equation (2.2) is a fixed-point equation

$$u_q(\cdot; d) = u^i(\cdot; d) + L_q u_q(\cdot; d) \quad \text{in } D$$

for the total field $u_q(\cdot; d)$, where the linear operator $L_q : L^2(D) \rightarrow L^2(D)$ is defined by

$$(L_q f)(x) := k^2 \int_D q(y) f(y) \Phi(x-y) \, dy, \quad x \in D. \quad (2.9)$$

If the operator norm $\|L_q\|$ is strictly less than one, then the solution to (2.2) can be written as

$$u_q(\cdot; d) = u^i(\cdot; d) + \sum_{l=1}^{\infty} (L_q)^l u^i(\cdot; d) \quad \text{in } D. \quad (2.10)$$

This series is often called the *Born series*. It converges in $L^2(D)$ and uniformly with respect to the illumination direction $d \in S^1$. Sufficient conditions on k and q for this to hold have, e.g. been discussed in [33, 36, 43, 49]. For instance, (2.9) immediately implies that

$$\|L_q\|^2 \leq k^4 \int_D \int_D |q(y) \Phi(x-y)|^2 \, dy \, dx = \|L_q\|_{\text{HS}}^2 \quad (2.11)$$

(see [47, theorem VI.23]). The asymptotic behavior of the fundamental solution $\Phi(x-y)$ as $|x-y| \rightarrow 0$ shows that the right hand side of (2.11) is finite. In particular, L_q is a Hilbert–Schmidt operator, and the Born series converges when $\|L_q\|_{\text{HS}} < 1$, which we assume henceforth.

The Born series describes the different levels of multiple scattering of the incident wave $u^i(\cdot; d)$ at the scatterer. Accordingly, we denote its l th summand by

$$u_q^{s,(l)}(\cdot; d) := (L_q)^l u^i(\cdot; d),$$

and refer to it as the scattered field component associated to scattering processes of order $l \geq 1$ on q . Substituting (2.10) into (2.2) and extending the right hand side to all of \mathbb{R}^2 , we find that the far field pattern of $u_q^s(\cdot; d)$ satisfies

$$u_q^\infty(\hat{x}; d) = k^2 \sum_{l=1}^\infty \int_D q(y) e^{-ik\hat{x}\cdot y} \left((L_q)^{l-1} u^i(\cdot; d) \right)(y) dy, \quad \hat{x} \in S^1. \quad (2.12)$$

This series converges in $L^2(S^1)$ and uniformly with respect to $d \in S^1$. We write

$$u_q^{\infty, (l)}(\hat{x}; d) := k^{2l} \int_D \cdots \int_D q(y_l) \cdots q(y_1) \Phi(y_l - y_{l-1}) \cdots \Phi(y_2 - y_1) \\ \times e^{ik(d \cdot y_1 - \hat{x} \cdot y_l)} dy_1 \cdots dy_l, \quad \hat{x} \in S^1, \quad (2.13)$$

for the l th summand in (2.12). For later reference, we note that (2.13) implies that each $u_q^{\infty, (l)}$, $l \geq 1$, satisfies the reciprocity relation

$$u_q^{\infty, (l)}(\hat{x}; d) = u_q^{\infty, (l)}(-d; -\hat{x}), \quad \hat{x}, d \in S^1. \quad (2.14)$$

Recalling (2.4) we introduce far field operator components associated to scattering processes of order $l \geq 1$,

$$F_q^{(l)} : L^2(S^1) \rightarrow L^2(S^1), \quad \left(F_q^{(l)} g \right)(\hat{x}) := \int_{S^1} u_q^{\infty, (l)}(\hat{x}; d) g(d) ds(d), \quad (2.15)$$

and for any $p \geq 1$ we define the Born far field operator of order p by

$$F_q^{(\leq p)} : L^2(S^1) \rightarrow L^2(S^1), \quad \left(F_q^{(\leq p)} g \right)(\hat{x}) := \sum_{l=1}^p \left(F_q^{(l)} g \right)(\hat{x}). \quad (2.16)$$

Then (2.4) and (2.12) together with the realization of the Hilbert–Schmidt norm of an integral operator on $L^2(S^1)$ by the L^2 -norm of its kernel (see [47, theorem VI.23]) yields that $F_q = \sum_{l=1}^\infty F_q^{(l)} = \lim_{p \rightarrow \infty} F_q^{(\leq p)}$ in $\text{HS}(L^2(S^1))$.

2.4. Sparse approximations of far field operators

Assuming that the support of the scatterer is contained in a ball $B_R(c) \subseteq \mathbb{R}^2$ for some $c \in \mathbb{R}^2$ and $R > 0$, we show next that the components $F_q^{(l)}$ of the far field operator in the Born series have sparse approximations with respect to some suitably modulated Fourier bases.

To begin with, we suppose that $D \subseteq B_R(0)$, i.e. we have $c=0$. Denoting by $(e_n)_n := (e^{in \arg(\cdot)} / \sqrt{2\pi})_n$ the Fourier basis of $L^2(S^1)$, and substituting the Jacobi–Anger expansion (see, e.g. [14, p 75])

$$e^{\pm ik\hat{x}\cdot y} = \sum_{n \in \mathbb{Z}} (\pm i)^n e^{-in \arg y} J_n(k|y|) e^{in \arg \hat{x}}, \quad y \in \mathbb{R}^2, \hat{x} \in S^1, \quad (2.17)$$

into (2.13) twice shows that the far field component associated to scattering processes of order $l \geq 1$ satisfies

$$u_q^{\infty, (l)}(\hat{x}; d) = \sum_{m \in \mathbb{Z}} \sum_{n \in \mathbb{Z}} a_{m,n}^{(l)} e_m(\hat{x}) \overline{e_n(d)}, \quad \hat{x}, d \in S^1,$$

with

$$a_{m,n}^{(l)} = 2\pi k^{2l} (-i)^{m-n} \int_D \cdots \int_D q(y_l) \cdots q(y_1) \Phi(y_l - y_{l-1}) \cdots \Phi(y_2 - y_1) \times e^{-i(m \arg y_l - n \arg y_1)} J_m(k|y_l|) J_n(k|y_1|) dy_1 \cdots dy_l. \tag{2.18}$$

Since $(e_n)_n$ is a complete orthonormal system in $L^2(S^1)$, we obtain from (2.15), [47, theorem VI.23], and Parseval’s identity that $\|F_{q,\dots,q}^{(l)}\|_{\text{HS}} = \|u_q^{\infty,(l)}\|_{L^2(S^1 \times S^1)} = \|(a_{m,n}^{(l)})_{m,n}\|_{\ell^2 \times \ell^2}$. Furthermore, applying the Cauchy–Schwarz inequality l times shows that

$$|a_{m,n}^{(l)}| \leq 2\pi k^{2l} \|q\|_{L^\infty(D)} \|J_m(k|\cdot|)\|_{L^2(D)} \|J_n(k|\cdot|)\|_{L^2(D)} \|L_q\|_{\text{HS}}^{l-1} \tag{2.19}$$

for all $l \geq 1$, and for all $m, n \in \mathbb{Z}$. Since $D \subseteq B_R(0)$, the estimate (2.19) implies that the coefficients $(a_{m,n}^{(l)})_{m,n}$ are essentially supported in the index range $|m|, |n| \lesssim kR$, and decay superlinearly as a function of $|m|, |n| \in \mathbb{N}$ for $|m|, |n| \gtrsim kR$. In fact, formula (3.8) in [29] yields

$$k \|J_n(k|\cdot|)\|_{L^2(D)} \leq \|J_n(|\cdot|)\|_{L^2(B_{kR}(0))} \tag{2.20}$$

$$\leq b_0 |n|^{\frac{1}{3}} \left(1 + \frac{1}{2|n|}\right)^{\frac{|n|+1}{2}} \frac{kR}{|n|} \left(\left(\frac{kR}{|n|}\right)^2 e^{1 - \left(\frac{kR}{|n|}\right)^2}\right)^{\frac{|n|}{2}}, \quad \text{if } |n| \geq kR,$$

where the constant b_0 satisfies $b_0 \approx 0.7928$. In addition, it has been shown in [29] that

$$\lim_{kR \rightarrow \infty} \frac{\|J_{\lceil \nu kR \rceil}(|\cdot|)\|_{L^2(B_{kR}(0))}^2}{2kR} = \begin{cases} \sqrt{1 - \nu^2} & \text{if } \nu \leq 1, \\ 0 & \text{else,} \end{cases} \tag{2.21}$$

where $\lceil \nu kR \rceil$ denotes the smallest integer that is greater or equal to νkR . Numerical tests in [29] confirm that the values $\|J_n(|\cdot|)\|_{L^2(B_{kR}(0))}^2$ approach the asymptote $2\sqrt{(kR)^2 - n^2}$ already for moderate values of kR and decay quickly for $n \gtrsim kR$ (see also figure 1 below). Choosing $N \gtrsim kR$ this means that we may approximate

$$u_q^{\infty,(l)}(\hat{x}; d) \approx \sum_{|m| \leq N} \sum_{|n| \leq N} a_{m,n}^{(l)} e_m(\hat{x}) \overline{e_n(d)}, \quad \hat{x}, d \in S^1. \tag{2.22}$$

Substituting (2.22) into (2.15) we obtain that

$$\left(F_q^{(l)} g\right)(\hat{x}) \approx \sum_{|m| \leq N} \sum_{|n| \leq N} a_{m,n}^{(l)} e_m(\hat{x}) \int_{S^1} g(d) \overline{e_n(d)} ds(d), \quad \hat{x} \in S^1, \tag{2.23}$$

is a reasonable approximation.

Example 2.3. To illustrate this sparse approximation, we consider the example $q = \chi_{B_R(0)}$. Then, the Fourier coefficients $(a_{m,n}^{(1)})_{m,n}$ from (2.18) with $l = 1$ satisfy

$$a_{m,n}^{(1)} = 2\pi k^2 (-i)^{m-n} \int_0^R J_m(kr) J_n(kr) r dr \int_0^{2\pi} e^{-i(m-n)\varphi} d\varphi$$

$$= \begin{cases} 2\pi \|J_n(|\cdot|)\|_{L^2(B_{kR}(0))}^2 & \text{if } n = m, \\ 0 & \text{else.} \end{cases}$$

Recalling (2.21), this shows that the cut-off parameter N in (2.23) cannot be chosen smaller than kR . \diamond

We define the finite dimensional subspace $\mathcal{V}_N \subseteq \text{HS}(L^2(S^1))$ by

$$\mathcal{V}_N := \left\{ G \in \text{HS}(L^2(S^1)) \mid Gg = \sum_{|m| \leq N} \sum_{|n| \leq N} a_{m,n} \mathbf{e}_m \langle g, \mathbf{e}_n \rangle_{L^2(S^1)} \right\}. \quad (2.24)$$

Still assuming that $N \gtrsim kR$, we refer to \mathcal{V}_N as the subspace of *non-evanescent far field operators* associated to scatterers supported in $B_R(0)$. Let $\mathcal{P}_N : \text{HS}(L^2(S^1)) \rightarrow \text{HS}(L^2(S^1))$ denote the orthogonal projection onto \mathcal{V}_N . Then the approximation error can be estimated as follows.

Lemma 2.4. *Let $q \in L^\infty(D)$ with $q > -1$ in D and $D \subseteq B_R(0)$. Then, for $l \geq 1$,*

$$\|F_q^{(l)} - \mathcal{P}_N F_q^{(l)}\|_{\text{HS}} \leq (2\pi)^{\frac{3}{2}} kR \|q\|_{L^\infty(D)} \|L_q\|_{\text{HS}}^{l-1} \left(\sum_{|n| > N} \|J_n(|\cdot|)\|_{L^2(B_{kR}(0))}^2 \right)^{\frac{1}{2}}. \quad (2.25)$$

Proof. Using Parseval’s identity we find that

$$\|F_q^{(l)} - \mathcal{P}_N F_q^{(l)}\|_{\text{HS}}^2 = \sum_{|m| > N} \sum_{n \in \mathbb{Z}} |a_{m,n}^{(l)}|^2 + \sum_{m \in \mathbb{Z}} \sum_{|n| > N} |a_{m,n}^{(l)}|^2 - \sum_{|m| > N} \sum_{|n| > N} |a_{m,n}^{(l)}|^2.$$

Substituting (2.19) and observing that

$$\sum_{n \in \mathbb{Z}} \|J_n(|\cdot|)\|_{L^2(B_{kR}(0))}^2 = \pi R^2$$

(see [29, lemma SM1.1]) yields (2.25). □

The last term on the right hand side can be further estimated by means of (2.20). We note that [18, (10.22.5)] shows that

$$\|J_n(|\cdot|)\|_{L^2(B_{kR}(0))}^2 = \pi (kR)^2 (J_n^2(kR) - J_{n-1}(kR)J_{n+1}(kR)), \quad n \in \mathbb{Z}.$$

In figure 1 we present plots of $\sum_{|n|=N+1}^{1000} \|J_n(|\cdot|)\|_{L^2(B_{kR}(0))}^2$ as a function of $N \in \mathbb{N}$ for $kR = 10$ (left) and for $kR = 100$ (right). The superlinear decay for $N \gtrsim kR$ is clearly visible.

Remark 2.5. Recalling (2.12), we find that the Fourier coefficients $(a_{m,n})_{m,n}$ of the full far field pattern satisfy $a_{m,n} = \sum_{l=1}^\infty a_{m,n}^{(l)}$. The estimates for $|a_{m,n}^{(l)}|$ in (2.19) and (2.20) show that $|a_{m,n}|$ is also decaying superlinearly for $|m|, |n| \gtrsim kR$. Thus also the full far field operator F_q has a sparse approximation

$$(F_q g)(\hat{x}) \approx \sum_{|m| \leq N} \sum_{|n| \leq N} a_{m,n} \mathbf{e}_m(\hat{x}) \int_{S^1} g(d) \overline{\mathbf{e}_n(d)} \, ds(d), \quad \hat{x} \in S^1, \quad (2.26)$$

with $N \gtrsim kR$. ◇

Remark 2.6. The reciprocity principle (2.14) gives that, for $l \geq 1$ and $\hat{x}, d \in S^1$,

$$\sum_{m \in \mathbb{Z}} \sum_{n \in \mathbb{Z}} a_{m,n}^{(l)} \mathbf{e}_m(\hat{x}) \overline{\mathbf{e}_n(d)} = \sum_{m \in \mathbb{Z}} \sum_{n \in \mathbb{Z}} (-1)^{m-n} a_{-n,-m}^{(l)} \mathbf{e}_m(\hat{x}) \overline{\mathbf{e}_n(d)}. \quad (2.27)$$

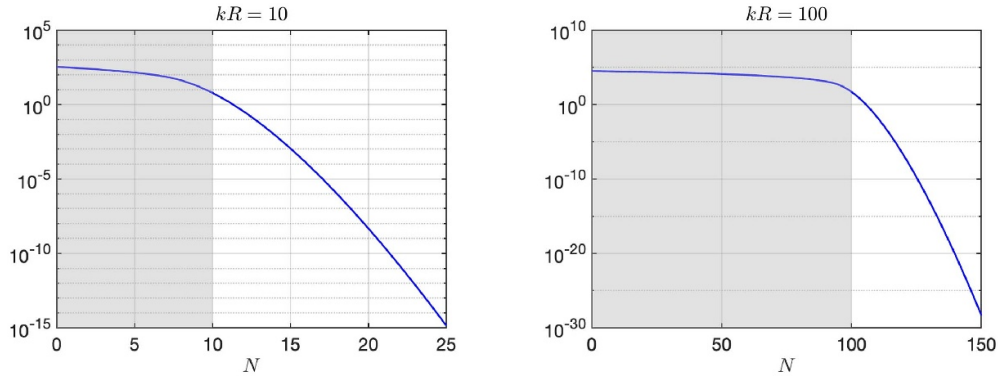


Figure 1. Plots of factor $\sum_{|n|>N} \|J_n(|\cdot|)\|_{L^2(B_{kR}(0))}^2$ in (2.25) as function of $N \in \mathbb{N}$ for $kR = 10$ (left) and for $kR = 100$ (right).

In particular,

$$a_{m,n}^{(l)} = (-1)^{m-n} a_{-n,-m}^{(l)}, \quad m, n \in \mathbb{Z}. \tag{2.28}$$

It would be possible to include (2.28) in the definition of the subspace \mathcal{V}_N to obtain even sparser representations of non-evanescent far field operators associated to scatterers supported in $B_R(0)$. We will comment on this further in remarks 3.11 and 3.17 below.

By (2.3) the formula (2.28) is also true for the Fourier coefficients $a_{m,n}$, $m, n \in \mathbb{Z}$, of the full far field pattern u_q^∞ . \diamond

If $D \subseteq B_R(c)$ for some $c \in \mathbb{R}^2$ with $c \neq 0$, then we can use the translation operator \mathcal{T}_c from (2.8) to shift the scatterer into the origin. Recalling (2.13), the kernel of the integral representation of $\mathcal{T}_c F_q^{(l)}$ is given by

$$k^{2l} \int_D \cdots \int_D q(y_l) \cdots q(y_1) \Phi(y_l - y_{l-1}) \cdots \Phi(y_2 - y_1) e^{ik(d \cdot (y_l - c) - \widehat{x} \cdot (y_l - c))} dy_1 \cdots dy_l,$$

which is the same as $u_{q_c, \dots, q_c}^{\infty, (l)}(\widehat{x}; d)$ (see also (2.6)). Now proceeding as in the special case $c = 0$, we find that $\mathcal{T}_c F_q^{(l)}$ has a sparse approximation

$$\left(\mathcal{T}_c F_q^{(l)} g\right)(\widehat{x}) \approx \sum_{|m| \leq N} \sum_{|n| \leq N} a_{m,n}^{(l)} \mathbf{e}_m \int_{S^1} g(d) \overline{\mathbf{e}_n(d)} ds(d), \quad \widehat{x} \in S^1,$$

in \mathcal{V}_N from (2.24) with $N \gtrsim kR$. Applying (2.8), we define the subspace $\mathcal{V}_N^c \subseteq \text{HS}(L^2(S^1))$ of non-evanescent far field operators associated to scatterers supported in $B_R(c)$ by

$$\mathcal{V}_N^c := \left\{ G \in \text{HS}(L^2(S^1)) \mid Gg = \sum_{|m| \leq N} \sum_{|n| \leq N} a_{m,n} e^{ikc \cdot (\cdot)} \mathbf{e}_m \langle g, e^{ikc \cdot (\cdot)} \mathbf{e}_n \rangle_{L^2(S^1)} \right\}, \tag{2.29}$$

i.e. $\mathcal{V}_N^c = \{G \in \text{HS}(L^2(S^1)) \mid \mathcal{T}_c G \in \mathcal{V}_N\}$. We call $(e^{ikc \cdot (\cdot)} \mathbf{e}_n)_n$ a modulated Fourier basis of $L^2(S^1)$, and accordingly the coefficients $(a_{m,n})_{m,n}$ in associated expansions as in (2.29) are called modulated Fourier coefficients. Let $\mathcal{P}_N^c : \text{HS}(L^2(S^1)) \rightarrow \text{HS}(L^2(S^1))$ denote the orthogonal projection onto \mathcal{V}_N^c . Then the error estimate (2.25) carries over.

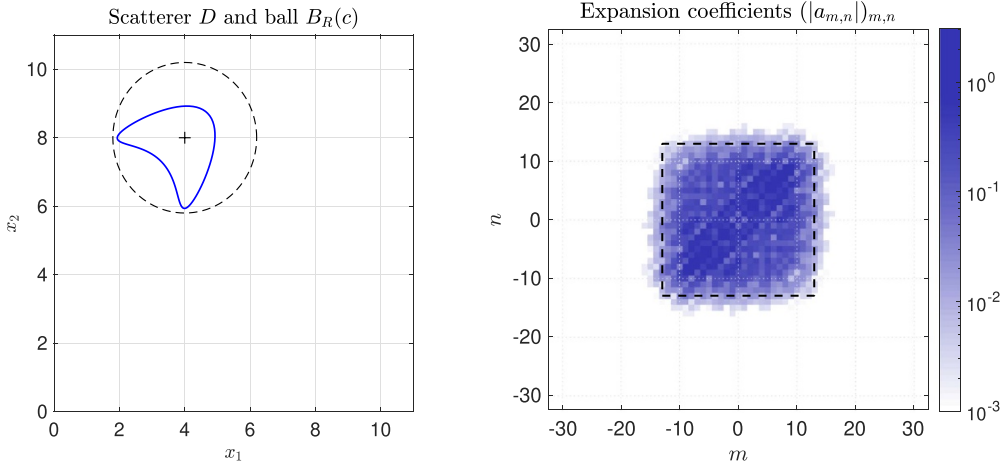


Figure 2. Left: support of scatterer D (solid) and ball $B_R(c)$ (dashed). Right: absolute values of modulated Fourier coefficients $(a_{m,n})_{m,n}$ of far field operator F_q at $k=5$. Dashed square corresponds to coefficients used by sparse approximation of F_q in \mathcal{V}_N^c with $N=13$.

Lemma 2.7. Let $q \in L^\infty(D)$ with $q > -1$ in D and $D \subseteq B_R(c)$. Then, for $l \geq 1$,

$$\|F_q^{(l)} - \mathcal{P}_N^c F_q^{(l)}\|_{\text{HS}} \leq (2\pi)^{\frac{3}{2}} kR \|q\|_{L^\infty(D)} \|L_q\|_{\text{HS}}^{l-1} \left(\sum_{|n| > N} \|J_n(|\cdot|)\|_{L^2(B_{kR}(0))}^2 \right)^{\frac{1}{2}}. \quad (2.30)$$

The upper bound on the right hand side of (2.30) decays quickly for $N \gtrsim kR$ (see figure 1). The same reasoning that led to (2.26) shows that the Born far field operator $F_q^{(\leq p)}$ of order $p \geq 1$ and also the full far field operator F_q have sparse approximations in \mathcal{V}_N^c .

Example 2.8. We illustrate our findings by a numerical example with $q = 2\chi_D$ for D as shown in figure 2(left). We use $k=5$ and simulate far field patterns $u^\infty(\hat{x}_m; d_n)$ of solutions to (2.1) for $L=256$ equidistant observation and illumination directions on S^1 using a Nyström method (see [14, pp 91–96]). Accordingly, the matrix

$$F_q := \frac{2\pi}{L} [u^\infty(\hat{x}_m; d_n)]_{1 \leq m, n \leq L} \in \mathbb{C}^{L \times L},$$

approximates the far field operator F_q from (2.4).

The scatterer D is contained in the ball $B_R(c)$ of radius $R=2.2$ centered at $c=(4, 8)$, which is also shown in figure 2(left). A two-dimensional fast Fourier transform of the shifted far field pattern $(e^{-ikc \cdot (d_n - \hat{x}_m)} u_q^\infty(\hat{x}_m; d_n))_{m,n} \in \mathbb{C}^{L \times L}$ yields an approximation of the modulated Fourier coefficients $(a_{m,n})_{m,n}$ of F_q with respect to the modulated Fourier basis $(e^{ikc \cdot (\cdot)} \mathbf{e}_n)_n$ of $L^2(S^1)$. In figure 2(right) the absolute values of these expansion coefficients are plotted in a logarithmic scale. It is confirmed that these coefficients are essentially supported in a square $[-N, N]^2$ with $N \gtrsim kR=11$. The dashed square in figure 2(right) corresponds to $N=13$. \diamond

3. Far field operator splitting

We consider the inverse problem (a) introduced in section 2.1. Suppose that the scatterer consists of two well-separated components, i.e. $D = D_1 \cup D_2$ for some $D_1, D_2 \subseteq \mathbb{R}^2$ and $D_j \subseteq B_{R_j}(c_j)$, $j = 1, 2$, with $c_1, c_2 \in \mathbb{R}^2$ and $R_1, R_2 > 0$ such that $|c_1 - c_2| > R_1 + R_2$. Let $q_1 := q|_{D_1}$ and $q_2 := q|_{D_2}$ denote the contrast functions of these two components. Then, each summand in the Born series (2.12) can be further decomposed. Recalling (2.13) we have, for $l \geq 1$,

$$u_q^{\infty, (l)}(\hat{x}; d) = \sum_{j_1=1}^2 \cdots \sum_{j_l=1}^2 u_{q_{j_1}, \dots, q_{j_l}}^{\infty, (l)}(\hat{x}; d), \quad \hat{x}, d \in S^1,$$

with

$$u_{q_{j_1}, \dots, q_{j_l}}^{\infty, (l)}(\hat{x}; d) := k^{2l} \int_{D_{j_1}} \cdots \int_{D_{j_l}} q_{j_1}(y_1) \cdots q_{j_l}(y_l) \Phi(y_l - y_{l-1}) \cdots \Phi(y_2 - y_1) e^{ik(d \cdot y_1 - \hat{x} \cdot y_l)} dy_1 \cdots dy_l, \\ \hat{x}, d \in S^1, j_1, \dots, j_l \in \{1, 2\}. \quad (3.1)$$

As indicated by our notation, the term $u_{q_{j_1}, \dots, q_{j_l}}^{\infty, (l)}$ describes the component of the far field pattern associated to the part of the scattered wave that results from l scattering processes starting at q_{j_1} , followed by q_{j_2} and so forth, until q_{j_l} . We note that these far field components satisfy the reciprocity relation

$$u_{q_{j_1}, \dots, q_{j_l}}^{\infty, (l)}(\hat{x}; d) = u_{q_{j_1}, \dots, q_{j_l}}^{\infty, (l)}(-d; -\hat{x}), \quad \hat{x}, d \in S^1. \quad (3.2)$$

Remark 3.1. Denoting by $(a_{m,n}^{(l)})_{m,n}$ and $(b_{m,n}^{(l)})_{m,n}$ the Fourier coefficients of $u_{q_{j_1}, \dots, q_{j_l}}^{\infty, (l)}$ and $u_{q_{j_1}, \dots, q_{j_l}}^{\infty, (l)}$, respectively, the same calculation as in (2.27), using (3.2) instead of (2.14), shows that

$$a_{m,n}^{(l)} = (-1)^{m-n} b_{-n, -m}^{(l)}, \quad m, n \in \mathbb{Z}. \quad (3.3)$$

◇

We define for $l \geq 1$ the far field operator components

$$F_{q_{j_1}, \dots, q_{j_l}}^{(l)} : L^2(S^1) \rightarrow L^2(S^1), \quad \left(F_{q_{j_1}, \dots, q_{j_l}}^{(l)} g\right)(\hat{x}) := \int_{S^1} u_{q_{j_1}, \dots, q_{j_l}}^{\infty, (l)}(\hat{x}; d) g(d) ds(d).$$

Therewith, we rewrite the Born far field operator of order p from (2.16) as

$$F_q^{(\leq p)} = F_{q_1}^{(\leq p)} + F_{q_2}^{(\leq p)} + \left(\sum_{l=1}^p \sum_{(j_1, \dots, j_l) \in \{1, 2\}^l \setminus (\{1\}^l \cup \{2\}^l)} F_{q_{j_1}, \dots, q_{j_l}}^{(l)} \right). \quad (3.4)$$

Remark 3.2. In the special case when $p = 1$ (i.e. Born approximation of order one, neglecting multiple scattering) the expansion (3.4) reduces to

$$F_q^{(\leq 1)} = F_{q_1}^{(\leq 1)} + F_{q_2}^{(\leq 1)}, \quad (3.5)$$

while for $p = 2$ (i.e. Born approximation of order two, including multiple scattering of order one) we obtain that

$$F_q^{(\leq 2)} = F_{q_1}^{(\leq 2)} + F_{q_2}^{(\leq 2)} + \left(F_{q_1, q_2}^{(2)} + F_{q_2, q_1}^{(2)} \right), \tag{3.6}$$

and for $p = 3$ (i.e. Born approximation of order three, including multiple scattering up to order two) the expansion (3.4) reads

$$F_q^{(\leq 3)} = F_{q_1}^{(\leq 3)} + F_{q_2}^{(\leq 3)} + \left(F_{q_1, q_2}^{(2)} + F_{q_2, q_1}^{(2)} + F_{q_1, q_1, q_2}^{(3)} + F_{q_1, q_2, q_1}^{(3)} + F_{q_1, q_2, q_2}^{(3)} + F_{q_2, q_1, q_1}^{(3)} + F_{q_2, q_1, q_2}^{(3)} + F_{q_2, q_2, q_1}^{(3)} \right). \tag{3.7}$$

The Born far field operators $F_q^{(\leq p)}$, $p = 1, 2, 3$, on the left hand sides of (3.5)–(3.7) are increasingly accurate approximations of the far field operator F_q corresponding to the system of two scatterers, while the first two terms $F_{q_1}^{(\leq p)}$ and $F_{q_2}^{(\leq p)}$, $p = 1, 2, 3$, on the right hand sides of (3.5)–(3.7) approximate the far field operators F_{q_1} and F_{q_2} corresponding to the two individual scatterers in D_1 and D_2 increasingly well. On the other hand, the terms in brackets on the right hand side of (3.6) and (3.7) approximate multiple scattering effects. The goal of far field operator splitting is to recover approximations of F_{q_1} and F_{q_2} from F_q . To this end we will split F_q into three components, two corresponding to the first two terms on the right hand side of (3.4) (or (3.5)–(3.7)), and one corresponding to the terms in brackets on the right hand side of these equations. Considering higher order Born approximations makes sense, because it gives better approximations of F_{q_1} and F_{q_2} . \diamond

We have already seen in lemma 2.7 that the far field operator components $F_{q_1}^{(\leq p)}$ and $F_{q_2}^{(\leq p)}$ in (3.4) have sparse approximations in the subspaces $\mathcal{V}_{N_1}^{c_1}$ and $\mathcal{V}_{N_2}^{c_2}$ with $N_1 \gtrsim kR_1$ and $N_2 \gtrsim kR_2$, respectively. In fact, the same reasoning shows that any term on the right hand side of (3.4) that is of the form $F_{q_1, q_{j_2}, \dots, q_{j_{l-1}}, q_1}^{(l)}$ or $F_{q_2, q_{j_2}, \dots, q_{j_{l-1}}, q_2}^{(l)}$, i.e. the first and the last interaction takes place at the same component of the scatterer, can be well approximated in $\mathcal{V}_{N_1}^{c_1}$ or $\mathcal{V}_{N_2}^{c_2}$, respectively, (see also lemma 3.4 below). To obtain sparse approximations of the remaining terms on the right hand side of (3.4), which are all of the form $F_{q_1, q_{j_2}, \dots, q_{j_{l-1}}, q_2}^{(l)}$ or $F_{q_2, q_{j_2}, \dots, q_{j_{l-1}}, q_1}^{(l)}$, we introduce for $M, N \in \mathbb{N}$ the finite dimensional subspace

$$\mathcal{V}_{M, N} := \left\{ G \in \text{HS}(L^2(S^1)) \mid Gg = \sum_{|m| \leq M} \sum_{|n| \leq N} a_{m, n} \mathbf{e}_m \langle g, \mathbf{e}_n \rangle_{L^2(S^1)} \right\}.$$

We note that $\mathcal{V}_{N, N} = \mathcal{V}_N$ from (2.24). Furthermore, we define for $b, c \in \mathbb{R}^2$ the *generalized translation operator*

$$\mathcal{T}_{b, c} : \text{HS}(L^2(S^1)) \rightarrow \text{HS}(L^2(S^1)), \quad \mathcal{T}_{b, c} G := T_b \circ G \circ T_{-c}, \tag{3.8}$$

where T_b and T_{-c} are defined as in (2.7). Then $\mathcal{T}_{c, c} = \mathcal{T}_c$ from (2.8).

Lemma 3.3. *Let $b, c \in \mathbb{R}^2$. The operator $\mathcal{T}_{b, c} \in \mathcal{L}(\text{HS}(L^2(S^1)))$ is unitary with $\mathcal{T}_{b, c}^* = \mathcal{T}_{-b, -c}$.*

Proof. For any $G, H \in \text{HS}(L^2(S^1))$ the definitions (2.7) and (3.8) imply that

$$\langle \mathcal{T}_{b, c} G, H \rangle_{\text{HS}} = \text{tr}((T_b G T_{-c})^* H) = \text{tr}(T_{-b} H T_c G^*) = \text{tr}(G^* T_{-b} H T_c) = \langle G, \mathcal{T}_{-b, -c} H \rangle_{\text{HS}}.$$

This shows that $\mathcal{T}_{b, c}^* = \mathcal{T}_{-b, -c}$, which is the same as $\mathcal{T}_{b, c}^{-1}$. \square

Substituting the Jacobi–Anger expansion (2.17) in (3.1) and proceeding as in section 2.4, we find that terms of the form $\mathcal{T}_{c_1, c_2} F_{q_1, q_2, \dots, q_{j_1-1}, q_2}^{(l)}$ and $\mathcal{T}_{c_2, c_1} F_{q_2, q_2, \dots, q_{j_1-1}, q_1}^{(l)}$ have sparse approximations in \mathcal{V}_{N_1, N_2} and \mathcal{V}_{N_2, N_1} with $N_1 \gtrsim kR_1$ and $N_2 \gtrsim kR_2$, respectively. Accordingly, we define

$$\mathcal{V}_{M, N}^{b, c} := \left\{ G \in \text{HS}(L^2(S^1)) \mid Gg = \sum_{|m| \leq M} \sum_{|n| \leq N} a_{m, n} e^{ikb \cdot (\cdot)} \mathbf{e}_m \langle g, \mathbf{e}_n \rangle_{L^2(S^1)} \right\}, \quad (3.9)$$

i.e. $\mathcal{V}_{M, N}^{b, c} = \{G \in \text{HS}(L^2(S^1)) \mid \mathcal{T}_{b, c} G \in \mathcal{V}_{M, N}\}$. We note that $\mathcal{V}_{N, N}^{c, c} = \mathcal{V}_N^c$ from (2.29). Then, $F_{q_1, q_2, \dots, q_{j_1-1}, q_2}^{(l)}$ and $F_{q_2, q_2, \dots, q_{j_1-1}, q_1}^{(l)}$ have sparse approximations in $\mathcal{V}_{N_1, N_2}^{c_1, c_2}$ and $\mathcal{V}_{N_2, N_1}^{c_2, c_1}$ with $N_1 \gtrsim kR_1$ and $N_2 \gtrsim kR_2$, respectively. Denoting by $\mathcal{P}_{M, N}^{b, c} : \text{HS}(L^2(S^1)) \rightarrow \text{HS}(L^2(S^1))$ the orthogonal projection onto $\mathcal{V}_{M, N}^{b, c}$, the approximation error can be estimated similar to (2.25) and (2.30). To this end, we define $L_{q, j, l} : L^2(D_j) \rightarrow L^2(D_l)$ by

$$(L_{q, j, l} f)(x) := k^2 \int_{D_j} q(y) f(y) \Phi(x - y) dy, \quad x \in D_l.$$

Lemma 3.4. *Let $q \in L^\infty(D)$ with $q > -1$ in $D = D_1 \cup D_2$ and $D_j \subseteq B_{R_j}(c_j)$, $j = 1, 2$. Then, for $l \geq 1$ and $1 \leq j_1, \dots, j_l \leq 2$,*

$$\begin{aligned} & \|F_{q_{j_1}, \dots, q_{j_l}}^{(l)} - \mathcal{P}_{N_{j_1}, N_{j_l}}^{c_{j_1}, c_{j_l}} F_{q_{j_1}, \dots, q_{j_l}}^{(l)}\|_{\text{HS}} \\ & \leq 2\pi^{\frac{3}{2}} \|q_{j_l}\|_{L^\infty(D_{j_l})} \|L_{q, j_1, j_2}\|_{\text{HS}} \cdots \|L_{q, j_{l-1}, j_l}\|_{\text{HS}} \\ & \quad \times \left((kR_{j_1})^2 \sum_{|n| > N_{j_1}} \|J_n(|\cdot|)\|_{L^2(B_{kR_{j_1}}(0))}^2 + (kR_{j_l})^2 \sum_{|n| > N_{j_l}} \|J_n(|\cdot|)\|_{L^2(B_{kR_{j_l}}(0))}^2 \right)^{\frac{1}{2}}. \end{aligned} \quad (3.10)$$

The proof of this lemma is similar to the proof of lemma 2.4 and is therefore omitted. Recalling (2.20), (2.21) and figure 1, the right hand side of (3.10) is small as long as we choose $N_{j_1} \gtrsim kR_{j_1}$ and $N_{j_l} \gtrsim kR_{j_l}$.

Example 3.5. We consider a numerical example with $q = -0.5\chi_{D_1} + 2\chi_{D_2}$ for D_1 and D_2 as shown in figure 3(left). We choose $k = 5$ and approximate the far field component $u_{q_1, q_2}^{\infty, (2)}(\hat{x}_m; d_n)$ (cf (3.1)) for $L = 256$ equidistant observation and illumination directions on S^1 using trigonometric interpolation as described in [48, 50].

The scatterers D_1 and D_2 are contained in balls $B_{R_1}(c_1)$ and $B_{R_2}(c_2)$ of radius $R_1 = 2.2$ and $R_2 = 1.1$ centered at $c_1 = (4, 8)$ and $c_2 = (8, 2)$, respectively. These are also shown in figure 3(left). A two-dimensional fast Fourier transform of the shifted far field pattern $(e^{-ik(c_2 \cdot d_n - c_1 \cdot \hat{x}_m)} u_{q_1, q_2}^{\infty, (2)}(\hat{x}_m; d_n))_{m, n} \in \mathbb{C}^{L \times L}$ yields an approximation of the Fourier coefficients $(a_{m, n}^{(2)})_{m, n}$ of $\mathcal{T}_{c_1, c_2} F_{q_1, q_2}^{\infty, (2)}$. In figure 3(right) the absolute values of these expansion coefficients are plotted for $-32 \leq m, n \leq 32$ in a logarithmic scale. It is confirmed that these coefficients are essentially supported in a rectangle $[-N_1, N_1] \times [-N_2, N_2]$ with $N_1 \gtrsim kR_1 = 11$ and $N_2 \gtrsim kR_2 = 5.5$. The dashed rectangle in figure 3(right) corresponds to $N_1 = 13$ and $N_2 = 7$. \diamond

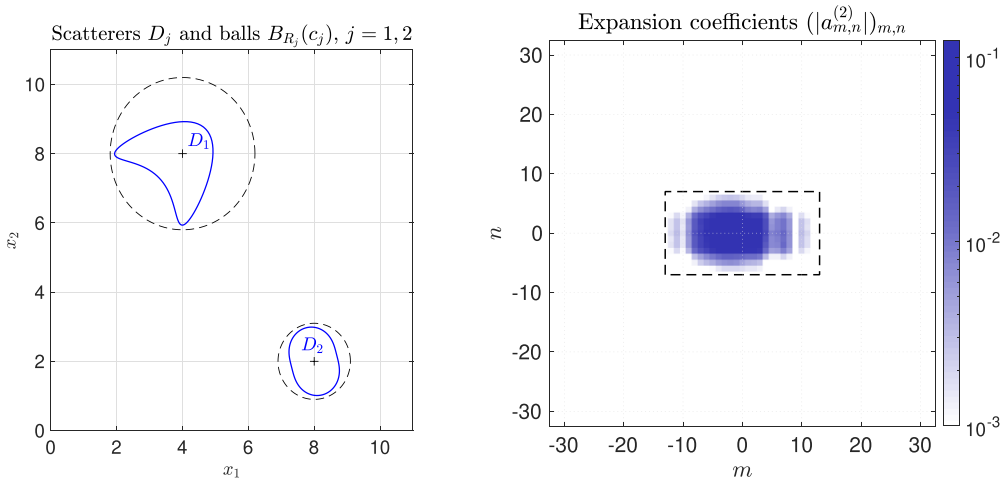


Figure 3. Left: supports of two scatterers D_1 and D_2 (solid) and balls $B_{R_1}(c_1)$ and $B_{R_2}(c_2)$ (dashed). Right: absolute values of modulated Fourier coefficients $(|a_{m,n}^{(2)}|)_{m,n}$ of $F_{q_1,q_2}^{(2)}$ at $k = 5$. Dashed rectangle corresponds to coefficients used by sparse approximation of $F_{q_1,q_2}^{(2)}$ in $\mathcal{V}_{N_1,N_2}^{c_1,c_2}$ with $N_1 = 13$ and $N_2 = 7$.

We will use the sparse representations of far field operator components ensured by lemmas 2.7 and 3.4 to develop numerical algorithms for the inverse problem (a) introduced in section 2.1 and to establish corresponding stability estimates. In section 3.1 we first neglect multiple scattering and use (3.5) as ansatz for far field operator splitting. This leads to concise stability estimates that we compare with earlier results from [25, 29]. A more accurate method taking into account multiple scattering is the subject of section 3.2.

3.1. Far field operator splitting in Born approximation of order 1

Given the far field operator F_q associated to two scattering objects with contrast functions q_1 and q_2 as defined at the beginning of section 3, we seek approximations $\tilde{F}_{q_1} \in \mathcal{V}_{N_1}^{c_1}$ and $\tilde{F}_{q_2} \in \mathcal{V}_{N_2}^{c_2}$ of the far field operators F_{q_1} and F_{q_2} , corresponding to the two components of the scatterer, satisfying the least squares problem

$$F_q \stackrel{\text{LS}}{=} \tilde{F}_{q_1} + \tilde{F}_{q_2} \quad \text{in } \text{HS}(L^2(S^1)). \tag{3.11}$$

In the following we discuss the conditioning of (3.11). To this end, we derive an upper bound on the cosine of the angle between $\mathcal{V}_{N_1}^{c_1}$ and $\mathcal{V}_{N_2}^{c_2}$, which immediately implies a bound the condition number of the splitting problem (3.11). This stability analysis has been motivated by similar results for the discrete and continuous one-dimensional Fourier transform in [19].

Remark 3.6. We will work with several different norms on $\text{HS}(L^2(S^1))$. To this end, we note that any Hilbert–Schmidt operator $G \in \text{HS}(L^2(S^1))$ has an integral representation

$$(Gf)(\hat{x}) = \int_{S^1} \kappa_G(\hat{x}; d) f(d) \, ds(d), \quad \hat{x} \in S^1, \tag{3.12}$$

for some $\kappa_G \in L^2(S^1 \times S^1)$ (see [47, theorem VI.23]), and the kernel κ_G can be expanded into a Fourier series

$$\kappa_G(\widehat{x}; d) = \sum_{m \in \mathbb{Z}} \sum_{n \in \mathbb{Z}} a_{m,n} e_m(\widehat{x}) \overline{e_n(d)}, \quad \widehat{x}, d \in S^1.$$

Accordingly, we use the notations

$$\|G\|_{L^p} := \|\kappa_G\|_{L^p(S^1 \times S^1)} \quad \text{and} \quad \|G\|_{\ell^p \times \ell^p} := \|(a_{m,n})_{m,n}\|_{\ell^p \times \ell^p}, \quad 1 \leq p \leq \infty.$$

We also observe that, for any $G, H \in \text{HS}(L^2(S^1))$,

$$\langle G, H \rangle_{\text{HS}} = \langle G, H \rangle_{L^2} = \langle G, H \rangle_{\ell^2 \times \ell^2} \tag{3.13}$$

(this can be seen as in the proof of [47, theorem VI.23] and using Parseval’s identity). Furthermore, we denote the area of the support of κ_G in $S^1 \times S^1$ by $\|G\|_{L^0}$, and the number of nonzero Fourier coefficients of κ_G by $\|G\|_{\ell^0 \times \ell^0}$. \diamond

Lemma 3.7. *Let $c \in \mathbb{R}^2, c \neq 0$, and let $\mathcal{T}_c : \text{HS}(L^2(S^1)) \rightarrow \text{HS}(L^2(S^1))$ be the translation operator in (2.8). Then, for all $1 \leq p \leq \infty$,*

$$\|\mathcal{T}_c G\|_{L^p} = \|G\|_{L^p}, \quad G \in \text{HS}(L^2(S^1)) \cap L^p(S^1 \times S^1), \tag{3.14}$$

and

$$\|\mathcal{T}_c G\|_{\ell^\infty \times \ell^\infty} \leq (k|c|)^{-\frac{2}{3}} \|G\|_{\ell^1 \times \ell^1}, \quad G \in \text{HS}(L^2(S^1)) \cap \ell^1 \times \ell^1. \tag{3.15}$$

If in addition $k|c| > 2(M + N + 1)$ for some $M, N \geq 1$, then¹

$$\|\mathcal{T}_c G\|_{\ell_M^\infty \times \ell_M^\infty} \leq (k|c|)^{-1} \|G\|_{\ell_N^1 \times \ell_N^1}, \quad G \in \text{HS}(L^2(S^1)) \cap \ell_N^1 \times \ell_N^1. \tag{3.16}$$

We also have that

$$\|\mathcal{T}_c G\|_{L^\infty} \leq \frac{1}{2\pi} \|\mathcal{T}_c G\|_{\ell^1 \times \ell^1}, \quad \mathcal{T}_c G \in \text{HS}(L^2(S^1)) \cap \ell^1 \times \ell^1. \tag{3.17}$$

Proof. The isometry property (3.14) follows immediately from the definition of the translation operator \mathcal{T}_c in (2.7) and (2.8).

To show (3.15), let $G \in \text{HS}(L^2(S^1)) \cap \ell^1 \times \ell^1$ and denote the associated kernel in the integral representation (3.12) by $\kappa_G \in L^2(S^1 \times S^1)$. The definitions (2.7) and (2.8) show that \mathcal{T}_c acts on κ_G as a multiplication operator,

$$(\mathcal{T}_c \kappa_G)(\widehat{x}; d) = e^{ik(\widehat{x}-d) \cdot c} \kappa_G(\widehat{x}; d), \quad \widehat{x}, d \in S^1.$$

Accordingly, it operates on the Fourier coefficients $(a_{m,n})_{m,n} \in \ell^2 \times \ell^2$ of κ_G as a convolution operator, and using (2.17) we obtain that the Fourier coefficients $(a_{m,n}^c)_{m,n}$ of $\mathcal{T}_c \kappa_G$ satisfy

$$a_{m,n}^c = \sum_{m' \in \mathbb{Z}} \sum_{n' \in \mathbb{Z}} a_{m-m', n-n'} \left(i^{m'-n'} e^{-i(m'-n') \arg c} J_{m'}(k|c|) J_{n'}(k|c|) \right), \quad m, n \in \mathbb{Z}.$$

¹ Here, $\ell_N^p := \{(c_n)_n \in \ell^p \mid \text{supp}(c_n)_n \subseteq [-N, N]\}$ for $1 \leq p \leq \infty$ and $N \in \mathbb{N}$.

Recalling that $|J_n(t)| < b/|t|^{\frac{1}{3}}$ for any $t \neq 0$ with $b \approx 0.7858$ (see [40, p 199]) we find that

$$\|\mathcal{T}_c G\|_{\ell^\infty \times \ell^\infty} \leq \| (J_n(k|c|))_n \|_{\ell^\infty}^2 \| (a_{m,n})_{m,n} \|_{\ell^1 \times \ell^1} \leq (k|c|)^{-\frac{2}{3}} \|G\|_{\ell^1 \times \ell^1}. \tag{3.18}$$

This shows (3.15).

Assuming that the support of $(a_{m,n})_{m,n}$ is contained in $[-N, N] \times [-N, N]$ we obtain similar to (3.18) that

$$\|\mathcal{T}_c G\|_{\ell_M^\infty \times \ell_M^\infty} \leq \| (J_n(k|c|))_n \|_{\ell_{M+N}^\infty}^2 \| (a_{m,n})_{m,n} \|_{\ell_N^1 \times \ell_N^1}.$$

Using the assumption that $k|c| > 2(M + N + 1)$ for some $M, N \geq 1$ and proceeding as in the proof of [29, theorem 4.6] using [39, theorem 2] gives $\sup_{|n| \leq M+N} |J_n(k|c|)| \leq b|c|^{-\frac{1}{2}}$ with $b \approx 0.7595$. Substituting this into (3.18) yields (3.16).

Finally, (3.17) follows from Hölder’s inequality, which gives

$$\|\mathcal{T}_c G\|_{L^\infty} = \|\mathcal{T}_c \kappa G\|_{L^\infty(S^1 \times S^1)} = \left\| \sum_{m \in \mathbb{Z}} \sum_{n \in \mathbb{Z}} a_{m,n}^c \mathbf{e}_m \overline{\mathbf{e}_n} \right\|_{L^\infty(S^1 \times S^1)} \leq \frac{1}{2\pi} \|\mathcal{T}_c G\|_{\ell^1 \times \ell^1}.$$

□

Next we derive upper bounds on the cosine of the angle between $\mathcal{V}_{N_1}^{c_1}$ and $\mathcal{V}_{N_2}^{c_2}$. This extends an uncertainty principle for far field patterns from [29, theorems 4.3 and 4.6] to far field operators. A related result on the correlation between the near fields radiated by two point sources located in c_1 and c_2 , respectively, has recently been analyzed in the high-frequency limit in [23, theorem 2.1].

Proposition 3.8. *Let $G \in \mathcal{V}_{N_1}^{c_1}$ and $H \in \mathcal{V}_{N_2}^{c_2}$ for some $c_1, c_2 \in \mathbb{R}^2$ and $N_1, N_2 \in \mathbb{N}$. Then,*

$$\frac{|\langle G, H \rangle_{\text{HS}}|}{\|G\|_{\text{HS}} \|H\|_{\text{HS}}} \leq \frac{\sqrt{\|\mathcal{T}_{c_1} G\|_{\ell^0 \times \ell^0} \|\mathcal{T}_{c_2} H\|_{\ell^0 \times \ell^0}}}{(k|c_2 - c_1|)^{\frac{2}{3}}} \leq \frac{(2N_1 + 1)(2N_2 + 1)}{(k|c_1 - c_2|)^{\frac{2}{3}}}. \tag{3.19}$$

If in addition $k|c_1 - c_2| > 2(N_1 + N_2 + 1)$ and $N_1, N_2 \geq 1$, then

$$\frac{|\langle G, H \rangle_{\text{HS}}|}{\|G\|_{\text{HS}} \|H\|_{\text{HS}}} \leq \frac{\sqrt{\|\mathcal{T}_{c_1} G\|_{\ell^0 \times \ell^0} \|\mathcal{T}_{c_2} H\|_{\ell^0 \times \ell^0}}}{k|c_2 - c_1|} \leq \frac{(2N_1 + 1)(2N_2 + 1)}{k|c_1 - c_2|}. \tag{3.20}$$

Proof. Using lemma 2.2, Hölder’s inequality, and (3.15) gives

$$\begin{aligned} |\langle G, H \rangle_{\text{HS}}| &= |\langle \mathcal{T}_{c_2} G, \mathcal{T}_{c_2} H \rangle_{\ell^2 \times \ell^2}| = \|\mathcal{T}_{c_2 - c_1} \mathcal{T}_{c_1} G\|_{\ell^\infty \times \ell^\infty} \|\mathcal{T}_{c_2} H\|_{\ell^1 \times \ell^1} \\ &\leq \frac{\sqrt{\|\mathcal{T}_{c_1} G\|_{\ell^0 \times \ell^0} \|\mathcal{T}_{c_2} H\|_{\ell^0 \times \ell^0}}}{(k|c_2 - c_1|)^{\frac{2}{3}}} \|\mathcal{T}_{c_1} G\|_{\ell^2 \times \ell^2} \|\mathcal{T}_{c_2} H\|_{\ell^2 \times \ell^2} \\ &\leq \frac{(2N_1 + 1)(2N_2 + 1)}{(k|c_2 - c_1|)^{\frac{2}{3}}} \|G\|_{\text{HS}} \|H\|_{\text{HS}}. \end{aligned}$$

If in addition $k|c_2 - c_1| > 2(N_1 + N_2 + 1)$ and $N_1, N_2 \geq 1$, then using (3.16) instead of (3.15) gives (3.20). □

In the following theorem F_q^δ denotes a noisy observation of a far field operator F_q corresponding to a scatterer $D = D_1 \cup D_2$ with two well-separated components $D_1 \subseteq B_{R_1}(c_1)$ and $D_2 \subseteq B_{R_2}(c_2)$. We assume that *a priori* information on the approximate location of these components is available, i.e. that the balls $B_{R_1}(c_1)$ and $B_{R_2}(c_2)$ are known. Accordingly, we choose $N_1 \gtrsim kR_1$ and $N_2 \gtrsim kR_2$ in the least squares problem (3.11) and compare the results for exact and noisy far field operators to establish a stability estimate. This generalizes the stability result for far field splitting from [29, theorem 5.3] to far field operator splitting.

Theorem 3.9. *Suppose that $F_q, F_q^\delta \in \text{HS}(L^2(S^1))$, and let $c_1, c_2 \in \mathbb{R}^2$ and $N_1, N_2 \in \mathbb{N}$ such that*

$$C := \frac{(2N_1 + 1)(2N_2 + 1)}{(k|c_1 - c_2|)^{\frac{3}{2}}} < 1.$$

Denote by $\tilde{F}_{q_1}, \tilde{F}_{q_2}$ and $\tilde{F}_{q_1}^\delta, \tilde{F}_{q_2}^\delta$ the solutions to the least squares problems

$$F_q \stackrel{\text{LS}}{=} \tilde{F}_{q_1} + \tilde{F}_{q_2}, \quad \tilde{F}_{q_1} \in \mathcal{V}_{N_1}^{c_1}, \tilde{F}_{q_2} \in \mathcal{V}_{N_2}^{c_2}, \quad (3.21a)$$

$$F_q^\delta \stackrel{\text{LS}}{=} \tilde{F}_{q_1}^\delta + \tilde{F}_{q_2}^\delta, \quad \tilde{F}_{q_1}^\delta \in \mathcal{V}_{N_1}^{c_1}, \tilde{F}_{q_2}^\delta \in \mathcal{V}_{N_2}^{c_2}, \quad (3.21b)$$

respectively. Then, for $j = 1, 2$,

$$\|\tilde{F}_{q_j} - \tilde{F}_{q_j}^\delta\|_{\text{HS}}^2 \leq (1 - C^2)^{-1} \|F_q - F_q^\delta\|_{\text{HS}}^2. \quad (3.22)$$

Remark 3.10. If $N_1, N_2 \geq 1$, $k|c_1 - c_2| > 2(N_1 + N_2 + 1)$ in theorem 3.9, and

$$\tilde{C} := \frac{(2N_1 + 1)(2N_2 + 1)}{k|c_1 - c_2|} < 1.$$

then (3.22) remains true with C replaced by \tilde{C} . \diamond

Proof. Denoting $F := F_q - F_q^\delta \in \text{HS}(L^2(S^1))$, $\tilde{F}_1 := \tilde{F}_{q_1} - \tilde{F}_{q_1}^\delta \in \mathcal{V}_{N_1}^{c_1}$ and $\tilde{F}_2 := \tilde{F}_{q_2} - \tilde{F}_{q_2}^\delta \in \mathcal{V}_{N_2}^{c_2}$, the least squares property (3.21) implies that

$$\|F\|_{\text{HS}}^2 = \|\tilde{F}_1 + \tilde{F}_2\|_{\text{HS}}^2 + \|F - (\tilde{F}_1 + \tilde{F}_2)\|_{\text{HS}}^2 \geq \|\tilde{F}_1 + \tilde{F}_2\|_{\text{HS}}^2.$$

Therefore, using (3.19) and the arithmetic-geometric mean inequality yields

$$\|F\|_{\text{HS}}^2 \geq \|\tilde{F}_1\|_{\text{HS}}^2 + \|\tilde{F}_2\|_{\text{HS}}^2 - C^2 \|\tilde{F}_1\|_{\text{HS}}^2 - \|\tilde{F}_2\|_{\text{HS}}^2.$$

This shows (3.22).

To obtain the improved estimate stated in remark 3.10, one has to replace (3.19) by (3.20) in this calculation. \square

Remark 3.11. Including the reciprocity property (2.28), into the definition (2.29) of the subspaces of non-evanescent far field operators allows to improve the constants C and \tilde{C} in the stability estimates in theorem 3.9. In fact, any $G \in \mathcal{V}_N$ with

$$Gg = \sum_{|m| \leq N} \sum_{|n| \leq N} a_{m,n} \mathbf{e}_m \langle g, \mathbf{e}_n \rangle_{L^2(S^1)}, \quad g \in L^2(S^1),$$

that satisfies (2.28) can be rewritten as

$$Gg = \sum_{|m| \leq N} \sum_{n=-m}^N a_{m,n} \left(1 - \frac{1}{2} \delta_n^{-m} \right) \left(\mathbf{e}_m \langle g, \mathbf{e}_n \rangle_{L^2(S^1)} + (-1)^{n+m} \overline{\mathbf{e}_n} \langle g, \overline{\mathbf{e}_m} \rangle_{L^2(S^1)} \right).$$

Here, δ_n^{-m} denotes the Kronecker delta. Accordingly, we define for any $c \in \mathbb{R}^2$ and $N \in \mathbb{N}$ the finite dimensional subspace

$$\mathcal{W}_N^c := \{G \in \text{HS}(L^2(S^1)) \mid \mathcal{T}_c G \in \mathcal{W}_N\}, \quad (3.23)$$

with

$$\mathcal{W}_N := \left\{ G \in \text{HS}(L^2(S^1)) \mid \right. \quad (3.24)$$

$$\left. Gg = \sum_{|m| \leq N} \sum_{n=-m}^N a_{m,n} \left(1 - \frac{1}{2} \delta_n^{-m} \right) \left(\mathbf{e}_m \langle g, \mathbf{e}_n \rangle_{L^2(S^1)} + (-1)^{n+m} \overline{\mathbf{e}_n} \langle g, \overline{\mathbf{e}_m} \rangle_{L^2(S^1)} \right) \right\}.$$

Then $\mathcal{W}_N^c \subseteq \mathcal{V}_N^c$ and thus the first inequality in (3.19) and (3.20), respectively, remains valid. However, since $\|G\|_{\ell^0 \times \ell^0} \leq (2N+1)(N+1)$ for any $G \in \mathcal{W}_N$, only about half as many coefficients are required when using this representation compared to the representation in (2.29). Accordingly, given $c_1, c_2 \in \mathbb{R}^2$ and $N_1, N_2 \in \mathbb{N}$, and replacing $\mathcal{V}_{N_1}^{c_1}$ and $\mathcal{V}_{N_2}^{c_2}$ by $\mathcal{W}_{N_1}^{c_1}$ and $\mathcal{W}_{N_2}^{c_2}$ in the least squares problems (3.21) yields the improved constants

$$C := \frac{\sqrt{(2N_1+1)(N_1+1)(2N_2+1)(N_2+1)}}{(k|c_1 - c_2|)^{\frac{2}{3}}},$$

$$\tilde{C} := \frac{\sqrt{(2N_1+1)(N_1+1)(2N_2+1)(N_2+1)}}{k|c_1 - c_2|}$$

in the stability estimates in theorem 3.9. These constants are better by a factor of about 1/2. \diamond

Remark 3.12. Recalling (2.4) it would be possible to split the far field operator F_q corresponding to a scatterer $D = D_1 \cup D_2$ with two components into two far field operators corresponding to each scatterer D_1 and D_2 by splitting the far field patterns $u_q^\infty(\cdot; d)$ for each illumination direction $d \in S^1$ individually using the methods developed in [25, 28, 29]. However, comparing the stability estimate for least squares splitting of single far field patterns $u_q^\infty(\cdot; d)$ established in [29, theorem 5.3] with the stability estimate for least squares splitting of whole far field operators F_q in theorem 3.9 we find that the latter is more stable. The stability estimates in [29, theorem 5.3] and in theorem 3.9 are of the same structure but the constants C and \tilde{C} in theorem 3.9 are the squares of the corresponding constants in [29, theorem 5.3]. Taking into account the additional improvement that can be obtained by using the reciprocity principle as outlined in remark 3.11, this shows a significant advantage of the algorithms developed in this work. \diamond

3.2. Far field operator splitting in Born approximation of order 2

Next we include multiple scattering into the algorithm for far field operator splitting. The main idea is to replace the ansatz (3.5) in the least squares problem (3.11) by (3.6). We have already developed sparse representations of the additional components $F_{q_1, q_2}^{(2)}$ and $F_{q_2, q_1}^{(2)}$ in lemma 3.4.

We note that using higher order Born approximations such as, e.g. (3.7) does not work with our approach, because terms like $F_{q_1, q_2, q_1}^{(3)}$ and $F_{q_2, q_1, q_2}^{(3)}$ cannot be distinguished from $F_{q_1}^{(3B)}$ and $F_{q_2}^{(3B)}$, respectively, using the techniques at hand. Essentially, we can only characterize the first and the last scatterer that interacts with the far field operator components in (3.4).

Given the far field operator F_q associated to the two scattering objects with contrast functions q_1 and q_2 as defined at the beginning of section 3, we seek approximations $\tilde{F}_{q_1} \in \mathcal{V}_{N_1}^{c_1}$ and $\tilde{F}_{q_2} \in \mathcal{V}_{N_2}^{c_2}$ of the far field operators F_{q_1} and F_{q_2} , corresponding to the two components of the scatterer, satisfying the least squares problem

$$F_q \stackrel{\text{LS}}{=} \tilde{F}_{q_1} + \tilde{F}_{q_2} + \tilde{F}_{q_1, q_2} + \tilde{F}_{q_2, q_1} \quad \text{in HS}(L^2(S^1)) \tag{3.25}$$

for some $\tilde{F}_{q_1, q_2} \in \mathcal{V}_{N_1, N_2}^{c_1, c_2}$ and $\tilde{F}_{q_2, q_1} \in \mathcal{V}_{N_2, N_1}^{c_2, c_1}$. In the following we discuss the conditioning of (3.25).

Lemma 3.13. *Let $c_1, c_2 \in \mathbb{R}^2$, and let $\mathcal{T}_{c_1, c_2} : \text{HS}(L^2(S^1)) \rightarrow \text{HS}(L^2(S^1))$ be the generalized translation operator in (3.8). Then, for any $G \in \text{HS}(L^2(S^1)) \cap \ell^1 \times \ell^1$,*

$$\|\mathcal{T}_{c_1, c_2} G\|_{\ell^\infty \times \ell^\infty} \leq \begin{cases} (k^2 |c_1| |c_2|)^{-\frac{1}{3}} \|G\|_{\ell^1 \times \ell^1} & \text{if } c_1, c_2 \neq 0, \\ (k|c_1|)^{-\frac{1}{3}} \|G\|_{\ell^1 \times \ell^1} & \text{if } c_1 \neq 0, c_2 = 0, \\ (k|c_2|)^{-\frac{1}{3}} \|G\|_{\ell^1 \times \ell^1} & \text{if } c_1 = 0, c_2 \neq 0. \end{cases} \tag{3.26}$$

Proposition 3.14. *Suppose that $G \in \mathcal{V}_{N_1, N_2}^{c_1, c_2}$ and $H \in \mathcal{V}_{N'_1, N'_2}^{c'_1, c'_2}$ for some $c_1, c'_1, c_2, c'_2 \in \mathbb{R}^2$ and $N_1, N'_1, N_2, N'_2 \in \mathbb{N}$. Then,*

$$\frac{|\langle G, H \rangle_{\text{HS}}|}{\|G\|_{\text{HS}} \|H\|_{\text{HS}}} \leq \begin{cases} \frac{\sqrt{(2N_1+1)(2N_2+1)(2N'_1+1)(2N'_2+1)}}{(k|c_1-c'_1|)^{\frac{1}{3}}(k|c_2-c'_2|)^{\frac{1}{3}}} & \text{if } c_1 \neq c'_1 \text{ and } c_2 \neq c'_2, \\ \frac{\sqrt{(2N_1+1)(2N_2+1)(2N'_1+1)(2N'_2+1)}}{(k|c_1-c'_1|)^{\frac{1}{3}}} & \text{if } c_1 = c'_1 \text{ and } c_2 \neq c'_2, \\ \frac{\sqrt{(2N_1+1)(2N_2+1)(2N'_1+1)(2N'_2+1)}}{(k|c_2-c'_2|)^{\frac{1}{3}}} & \text{if } c_1 \neq c'_1 \text{ and } c_2 = c'_2. \end{cases} \tag{3.27}$$

The proofs of lemma 3.13 and proposition 3.14 are similar to the proof of lemma 3.7 and proposition 3.8 and are therefore omitted. In the following theorem we establish a stability result for the least squares problem (3.25) that is similar to theorem 3.9.

Theorem 3.15. *Suppose that $F_q, F_q^\delta \in \text{HS}(L^2(S^1))$, let $c_1, c_2 \in \mathbb{R}^2$ and $N_1, N_2 \in \mathbb{N}$, and define*

$$C := \frac{(2N_1 + 1)(2N_2 + 1)}{(k|c_1 - c_2|)^{\frac{2}{3}}}.$$

We assume that, for all $(j, l) \in \{1, 2\}^2$,

$$M_{j, l} := \sqrt{C} \left(\sqrt{C} + (2N_j + 1) + (2N_l + 1) \right) < 1.$$

Denote by $\tilde{F}_{q_1}, \tilde{F}_{q_2}, \tilde{F}_{q_1, q_2}, \tilde{F}_{q_2, q_1}$ and $\tilde{F}_{q_1}^\delta, \tilde{F}_{q_2}^\delta, \tilde{F}_{q_1, q_2}^\delta, \tilde{F}_{q_2, q_1}^\delta$ the solutions to the least squares problems

$$F_q \stackrel{\text{LS}}{=} \tilde{F}_{q_1} + \tilde{F}_{q_2} + \tilde{F}_{q_1, q_2} + \tilde{F}_{q_2, q_1}, \quad \tilde{F}_{q_j} \in \mathcal{V}_{N_j}^{c_j}, \tilde{F}_{q_j, q_l} \in \mathcal{V}_{N_j, N_l}^{c_j, c_l}, \quad (3.28a)$$

$$F_q^\delta \stackrel{\text{LS}}{=} \tilde{F}_{q_1}^\delta + \tilde{F}_{q_2}^\delta + \tilde{F}_{q_1, q_2}^\delta + \tilde{F}_{q_2, q_1}^\delta, \quad \tilde{F}_{q_j}^\delta \in \mathcal{V}_{N_j}^{c_j}, \tilde{F}_{q_j, q_l}^\delta \in \mathcal{V}_{N_j, N_l}^{c_j, c_l}, \quad (3.28b)$$

respectively. Then,

$$\|\tilde{F}_{q_j} - \tilde{F}_{q_j}^\delta\|_{\text{HS}}^2 \leq (1 - M_{j,j})^{-1} \|F_q - F_q^\delta\|_{\text{HS}}^2, \quad j = 1, 2. \quad (3.29)$$

To prove this result one can proceed similarly to the proof of theorem 3.9.

Remark 3.16. If $N_1, N_2 \geq 1$, $k|c_1 - c_2| > 2(N_1 + N_2 + 1)$ in theorem 3.15, and

$$\tilde{C} := \frac{(2N_1 + 1)(2N_2 + 1)}{k|c_1 - c_2|} < 1,$$

then (4.7) remains true with C replaced by \tilde{C} . This can be shown analogously to the improved estimate in remark 3.10. \diamond

Remark 3.17. Similar to remark 3.11, including the reciprocity properties (2.28) and (3.3) into the ansatz spaces for the least squares problems (4.6), the constants $M_{j,l}$, $(j, l) \in \{1, 2\}^2$, in theorem 3.15 can be improved by a factor of about $1/2$. Given $c_1, c_2 \in \mathbb{R}^2$ and $N_1, N_2 \in \mathbb{N}$, one needs to replace the subspaces $\mathcal{V}_{N_1}^{c_1}$ and $\mathcal{V}_{N_2}^{c_2}$ in (4.6) by $\mathcal{W}_{N_1}^{c_1}$ and $\mathcal{W}_{N_2}^{c_2}$ as defined in (3.23). Moreover, the unknowns $\tilde{F}_{q_1, q_2}, \tilde{F}_{q_2, q_1}$ and $\tilde{F}_{q_1, q_2}^\delta, \tilde{F}_{q_2, q_1}^\delta$, respectively, have to be combined into a single unknown using (3.3). \diamond

If *a priori* knowledge of the sizes R_j of the individual scatterers $D_j \subseteq B_{R_j}(c_j)$, $j = 1, 2$, which is required to determine the parameters $N_j \gtrsim kR_j$ of the ansatz spaces in the least squares formulation (3.25), is not available but at least the approximate positions c_1 and c_2 are known, then (3.25) can be replaced by an $\ell^1 \times \ell^1$ minimization problem. In theorem 3.18 below we present this approach and establish an associated stability result. As before, F_q^δ represents a noisy observation of a far field operator F_q corresponding to a scatterer $D = D_1 \cup D_2$ with two well-separated components $D_1 \subseteq B_{R_1}(c_1)$ and $D_2 \subseteq B_{R_2}(c_2)$. Accordingly, let

$$F_q \approx \tilde{F}_{q_1} + \tilde{F}_{q_2} + \tilde{F}_{q_1, q_2} + \tilde{F}_{q_2, q_1} \quad (3.30)$$

be an approximate decomposition of the exact far field operator with $\tilde{F}_{q_1} \in \mathcal{V}_{N_1}^{c_1}$, $\tilde{F}_{q_2} \in \mathcal{V}_{N_2}^{c_2}$, $\tilde{F}_{q_1, q_2} \in \mathcal{V}_{N_1, N_2}^{c_1, c_2}$, and $\tilde{F}_{q_2, q_1} \in \mathcal{V}_{N_2, N_1}^{c_2, c_1}$ for some $N_1 \gtrsim kR_1$ and $N_2 \gtrsim kR_2$, which could be the least squares solution of (3.25) but does not have to be computed. The bound $\delta_0 \geq 0$ in (3.31) describes the accuracy of this approximate solution, which in case of the least squares solution corresponds to the error of the second order Born approximation and projection errors as in (2.30) and (3.10). Now the optimization problem (3.33) seeks an approximate decomposition of the given noisy far field operator F_q^δ in the spaces $\mathcal{V}_{N_1}^{c_1}$, $\mathcal{V}_{N_2}^{c_2}$, $\mathcal{V}_{N_1, N_2}^{c_1, c_2}$, and $\mathcal{V}_{N_2, N_1}^{c_2, c_1}$ but without specifying $N_1, N_2 > 0$ in advance. Here, the assumption (3.32) guarantees that the approximate split (3.30) is feasible. The theorem gives a stability estimate for the solution of this minimization problem.

Theorem 3.18. Suppose that $F_q \in \text{HS}(L^2(S^1))$, let $c_1, c_2 \in \mathbb{R}^2$ and $N_1, N_2 \in \mathbb{N}$ such that for all $(j, l) \in \{1, 2\}^2$,

$$C_{j,l} := \frac{12(2N_j + 1)(2N_l + 1)}{(k|c_1 - c_2|)^{\frac{1}{3}}} < 1.$$

We assume that $\tilde{F}_{q_1} \in \mathcal{V}_{N_1}^{c_1}$, $\tilde{F}_{q_2} \in \mathcal{V}_{N_2}^{c_2}$, $\tilde{F}_{q_1, q_2} \in \mathcal{V}_{N_1, N_2}^{c_1, c_2}$, and $\tilde{F}_{q_2, q_1} \in \mathcal{V}_{N_2, N_1}^{c_2, c_1}$ are such that

$$\|F_q - (\tilde{F}_{q_1} + \tilde{F}_{q_2} + \tilde{F}_{q_1, q_2} + \tilde{F}_{q_2, q_1})\|_{\text{HS}} \leq \delta_0 \quad (3.31)$$

for some $\delta_0 \geq 0$. Moreover, suppose that $F_q^\delta \in \text{HS}(L^2(S^1))$ and $\delta \geq 0$ satisfy

$$\delta \geq \delta_0 + \|F_q - F_q^\delta\|_{\text{HS}} \quad (3.32)$$

and let $(\tilde{F}_{q_1}^\delta, \tilde{F}_{q_2}^\delta, \tilde{F}_{q_1, q_2}^\delta, \tilde{F}_{q_2, q_1}^\delta) \in \text{HS}(L^2(S^1))^4$ denote the solution to

$$\begin{aligned} \underset{F_{q_1}, \tilde{F}_{q_2}, \tilde{F}_{q_1, q_2}, \tilde{F}_{q_2, q_1}}{\text{minimize}} \quad & \|\mathcal{T}_{c_1} F_{q_1}\|_{\ell^1 \times \ell^1} + \|\mathcal{T}_{c_2} F_{q_2}\|_{\ell^1 \times \ell^1} + \|\mathcal{T}_{c_1, c_2} F_{q_1, q_2}\|_{\ell^1 \times \ell^1} + \|\mathcal{T}_{c_2, c_1} F_{q_2, q_1}\|_{\ell^1 \times \ell^1} \\ \text{subject to} \quad & \|F_q^\delta - (F_{q_1} + F_{q_2} + F_{q_1, q_2} + F_{q_2, q_1})\|_{\text{HS}} \leq \delta. \end{aligned} \quad (3.33)$$

Then,

$$\|\tilde{F}_{q_j} - \tilde{F}_{q_j}^\delta\|_{\text{HS}}^2 \leq (1 - C_{j,j})^{-1} 4\delta^2, \quad j = 1, 2.$$

Proof. We define $F := F_q - F_q^\delta$, $\tilde{F}_1 := \tilde{F}_{q_1} - \tilde{F}_{q_1}^\delta$, $\tilde{F}_2 := \tilde{F}_{q_2} - \tilde{F}_{q_2}^\delta$, $\tilde{F}_{1,2} := \tilde{F}_{q_1, q_2} - \tilde{F}_{q_1, q_2}^\delta$, and $\tilde{F}_{2,1} := \tilde{F}_{q_2, q_1} - \tilde{F}_{q_2, q_1}^\delta$. Moreover, we denote the $\ell^0 \times \ell^0$ support of $\mathcal{T}_{c_1} \tilde{F}_{q_1}$, $\mathcal{T}_{c_2} \tilde{F}_{q_2}$, $\mathcal{T}_{c_1, c_2} \tilde{F}_{q_1, q_2}$, and $\mathcal{T}_{c_2, c_1} \tilde{F}_{q_2, q_1}$ by W_1 , W_2 , $W_{1,2}$, and $W_{2,1}$, respectively, and the complements of the first two by W_1^c and W_2^c . We estimate, for $j \in \{1, 2\}$,

$$\begin{aligned} \|\mathcal{T}_{c_j} \tilde{F}_{q_j}^\delta\|_{\ell^1 \times \ell^1} &= \|\mathcal{T}_{c_j} (\tilde{F}_{q_j} + \tilde{F}_j)\|_{\ell^1 \times \ell^1} = \|\mathcal{T}_{c_j} (\tilde{F}_{q_j} + \tilde{F}_j)\|_{(\ell^1 \times \ell^1)(W_j)} + \|\mathcal{T}_{c_j} \tilde{F}_j\|_{(\ell^1 \times \ell^1)(W_j^c)} \\ &= \|\mathcal{T}_{c_j} (\tilde{F}_{q_j} + \tilde{F}_j)\|_{(\ell^1 \times \ell^1)(W_j)} + \|\mathcal{T}_{c_j} \tilde{F}_j\|_{\ell^1 \times \ell^1} - \|\mathcal{T}_{c_j} \tilde{F}_j\|_{(\ell^1 \times \ell^1)(W_j)} \\ &\geq \|\mathcal{T}_{c_j} \tilde{F}_{q_j}\|_{(\ell^1 \times \ell^1)(W_j)} + \|\mathcal{T}_{c_j} \tilde{F}_j\|_{\ell^1 \times \ell^1} - 2\|\mathcal{T}_{c_j} \tilde{F}_j\|_{(\ell^1 \times \ell^1)(W_j)} \end{aligned}$$

and we can do the same for $\tilde{F}_{q_l}^\delta$ with $j, l \in \{1, 2\}, j \neq l$. Together with (3.33) this gives

$$\begin{aligned} & \|\mathcal{T}_{c_1} \tilde{F}_1\|_{\ell^1 \times \ell^1} + \|\mathcal{T}_{c_2} \tilde{F}_2\|_{\ell^1 \times \ell^1} + \|\mathcal{T}_{c_1, c_2} \tilde{F}_{1,2}\|_{\ell^1 \times \ell^1} + \|\mathcal{T}_{c_2, c_1} \tilde{F}_{2,1}\|_{\ell^1 \times \ell^1} \\ & \leq 2(\|\mathcal{T}_{c_1} \tilde{F}_1\|_{(\ell^1 \times \ell^1)(W_1)} + \|\mathcal{T}_{c_2} \tilde{F}_2\|_{(\ell^1 \times \ell^1)(W_2)} \\ & \quad + \|\mathcal{T}_{c_1, c_2} \tilde{F}_{1,2}\|_{(\ell^1 \times \ell^1)(W_{1,2})} + \|\mathcal{T}_{c_2, c_1} \tilde{F}_{2,1}\|_{(\ell^1 \times \ell^1)(W_{2,1})}). \end{aligned} \quad (3.34)$$

Using (3.31)–(3.33) and (3.26) we obtain

$$\begin{aligned}
4\delta^2 &\geq \|\tilde{F}_1\|_{\text{HS}}^2 + \|\tilde{F}_2\|_{\text{HS}}^2 + \|\tilde{F}_{1,2}\|_{\text{HS}}^2 + \|\tilde{F}_{2,1}\|_{\text{HS}}^2 \\
&\quad - 2|\langle \tilde{F}_1, \tilde{F}_2 \rangle_{\text{HS}}| - 2|\langle \tilde{F}_1, \tilde{F}_{1,2} \rangle_{\text{HS}}| - 2|\langle \tilde{F}_1, \tilde{F}_{2,1} \rangle_{\text{HS}}| \\
&\quad - 2|\langle \tilde{F}_2, \tilde{F}_{1,2} \rangle_{\text{HS}}| - 2|\langle \tilde{F}_2, \tilde{F}_{2,1} \rangle_{\text{HS}}| - 2|\langle \tilde{F}_{1,2}, \tilde{F}_{2,1} \rangle_{\text{HS}}| \\
&\geq \|\tilde{F}_1\|_{\text{HS}}^2 + \|\tilde{F}_2\|_{\text{HS}}^2 + \|\tilde{F}_{1,2}\|_{\text{HS}}^2 + \|\tilde{F}_{2,1}\|_{\text{HS}}^2 \\
&\quad - \frac{2}{(k|c_1 - c_2|)^{\frac{2}{3}}} (\|\mathcal{T}_{c_1} \tilde{F}_1\|_{\ell^1 \times \ell^1} \|\mathcal{T}_{c_2} \tilde{F}_2\|_{\ell^1 \times \ell^1} + \|\mathcal{T}_{c_1, c_2} \tilde{F}_{1,2}\|_{\ell^1 \times \ell^1} \|\mathcal{T}_{c_2, c_1} \tilde{F}_{2,1}\|_{\ell^1 \times \ell^1}) \\
&\quad - \frac{2}{(k|c_1 - c_2|)^{\frac{2}{3}}} (\|\mathcal{T}_{c_1} \tilde{F}_1\|_{\ell^1 \times \ell^1} \|\mathcal{T}_{c_1, c_2} \tilde{F}_{1,2}\|_{\ell^1 \times \ell^1} + \|\mathcal{T}_{c_1} \tilde{F}_1\|_{\ell^1 \times \ell^1} \|\mathcal{T}_{c_2, c_1} \tilde{F}_{2,1}\|_{\ell^1 \times \ell^1} \\
&\quad\quad + \|\mathcal{T}_{c_2} \tilde{F}_2\|_{\ell^1 \times \ell^1} \|\mathcal{T}_{c_1, c_2} \tilde{F}_{1,2}\|_{\ell^1 \times \ell^1} + \|\mathcal{T}_{c_2} \tilde{F}_2\|_{\ell^1 \times \ell^1} \|\mathcal{T}_{c_2, c_1} \tilde{F}_{2,1}\|_{\ell^1 \times \ell^1}).
\end{aligned}$$

For $a_1, \dots, a_4 \geq 0$ a simple calculation shows that $\sum_i \sum_{j \neq i} a_i a_j \leq \frac{3}{4} (\sum_i a_i)^2 \leq 3 \sum_i a_i^2$. Together with (3.34) and the Cauchy Schwarz inequality this implies

$$\begin{aligned}
4\delta^2 &\geq \|\tilde{F}_1\|_{\text{HS}}^2 + \|\tilde{F}_2\|_{\text{HS}}^2 + \|\tilde{F}_{1,2}\|_{\text{HS}}^2 + \|\tilde{F}_{2,1}\|_{\text{HS}}^2 \\
&\quad - \frac{3}{4(k|c_1 - c_2|)^{\frac{2}{3}}} (\|\mathcal{T}_{c_1} \tilde{F}_1\|_{\ell^1 \times \ell^1} + \|\mathcal{T}_{c_2} \tilde{F}_2\|_{\ell^1 \times \ell^1} + \|\mathcal{T}_{c_1, c_2} \tilde{F}_{1,2}\|_{\ell^1 \times \ell^1} + \|\mathcal{T}_{c_2, c_1} \tilde{F}_{2,1}\|_{\ell^1 \times \ell^1})^2 \\
&\geq \|\tilde{F}_1\|_{\text{HS}}^2 + \|\tilde{F}_2\|_{\text{HS}}^2 + \|\tilde{F}_{1,2}\|_{\text{HS}}^2 + \|\tilde{F}_{2,1}\|_{\text{HS}}^2 \\
&\quad - \frac{3}{(k|c_1 - c_2|)^{\frac{2}{3}}} (\|\mathcal{T}_{c_1} \tilde{F}_1\|_{\ell^1 \times \ell^1(w_1)} + \|\mathcal{T}_{c_2} \tilde{F}_2\|_{\ell^1 \times \ell^1(w_2)} \\
&\quad\quad + \|\mathcal{T}_{c_1, c_2} \tilde{F}_{1,2}\|_{\ell^1 \times \ell^1(w_{1,2})} + \|\mathcal{T}_{c_2, c_1} \tilde{F}_{2,1}\|_{\ell^1 \times \ell^1(w_{2,1})})^2 \\
&\geq \|\tilde{F}_1\|_{\text{HS}}^2 + \|\tilde{F}_2\|_{\text{HS}}^2 + \|\tilde{F}_{1,2}\|_{\text{HS}}^2 + \|\tilde{F}_{2,1}\|_{\text{HS}}^2 \\
&\quad - \frac{3}{(k|c_1 - c_2|)^{\frac{2}{3}}} (|W_1|^{\frac{1}{2}} \|\tilde{F}_1\|_{\text{HS}} + |W_2|^{\frac{1}{2}} \|\tilde{F}_2\|_{\text{HS}} + |W_{1,2}|^{\frac{1}{2}} \|\tilde{F}_{1,2}\|_{\text{HS}} + |W_{2,1}|^{\frac{1}{2}} \|\tilde{F}_{2,1}\|_{\text{HS}})^2 \\
&\geq (1 - C_{1,1}) \|\tilde{F}_1\|_{\text{HS}}^2 + (1 - C_{2,2}) \|\tilde{F}_2\|_{\text{HS}}^2 + (1 - C_{1,2}) (\|\tilde{F}_{1,2}\|_{\text{HS}}^2 + \|\tilde{F}_{2,1}\|_{\text{HS}}^2).
\end{aligned}$$

□

The assumptions of theorem 3.18 are much more restrictive than the assumptions of theorem 3.15 and the stability estimate is worse, but the $\ell^1 \times \ell^1$ minimization algorithm requires less *a priori* information and our numerical results in section 5 suggest that both algorithms work comparably well.

Remark 3.19. Similar to remark 3.17 the reciprocity principle can be used to improve the constants $C_{j,l}$, $(j, l) \in \{1, 2\}^2$, in theorem 3.18 by a factor of about 1/2. ◇

4. Far field operator completion

We consider the inverse problem (b) introduced in section 2.1. Suppose that the scatterer $D \subseteq B_R(c)$ is contained in a ball of radius $R > 0$ centered at $c \in \mathbb{R}^2$, and that the far field pattern u_q^∞ cannot be observed on some subset $\Omega \subseteq S^1 \times S^1$. Without loss of generality we assume that Ω^c is symmetric in the sense of reciprocity, i.e. that $\Omega^c = \Omega^{c,r}$ with $\Omega^{c,r} := \{(-d, -\hat{x}) \mid (\hat{x}; d) \in \Omega^c\}$. Otherwise (2.3) can be used to extend the restricted far field

patterns from Ω^c to $\Omega^c \cup \Omega^{c,r}$. We define the infinite dimensional subspace

$$\mathcal{V}_\Omega := \left\{ G \in \text{HS}(L^2(S^1)) \mid Gg = \int_{S^1} \chi_\Omega(\cdot, d) \alpha(\cdot; d) g(d) \, ds(d), \alpha \in L^2(S^1 \times S^1) \right\}.$$

Given the restricted far field operator $F_q|_{\Omega^c}$ from (2.5) we seek approximations $\widetilde{F}_q^c \in \mathcal{V}_N^c$ and $\widetilde{B} \in \mathcal{V}_\Omega$ of the far field operator F_q and of its non-observable part $B := F_q|_{\Omega^c} - F_q$ satisfying the least squares problem

$$F_q|_{\Omega^c} \stackrel{\text{LS}}{=} \widetilde{F}_q^c + \widetilde{B} \quad \text{in } \text{HS}(L^2(S^1)). \quad (4.1)$$

The condition number of (4.1) is given by the cosecant of the angle between \mathcal{V}_N^c and \mathcal{V}_Ω , which can be estimated using upper bounds on the cosine of the angle between these two spaces.

Proposition 4.1. *Suppose that $G \in \mathcal{V}_N^c$ and $H \in \mathcal{V}_\Omega$ for some $c \in \mathbb{R}^2$, $N \in \mathbb{N}$, and $\Omega \subseteq S^1 \times S^1$. Then,*

$$\frac{|(G, H)_{\text{HS}}|}{\|G\|_{\text{HS}} \|H\|_{\text{HS}}} \leq \frac{(2N+1) \sqrt{|\Omega|}}{2\pi}. \quad (4.2)$$

Proof. Using (3.13), Hölder's inequality, (3.14) with $p = \infty$, and (3.17) yields

$$\begin{aligned} |(G, H)_{\text{HS}}| &= |(G, H)_{L^2}|\leq \|G\|_{L^\infty} \|H\|_{L^1} = \|\mathcal{T}_c G\|_{L^\infty} \|H\|_{L^1} \leq \frac{1}{2\pi} \|\mathcal{T}_c G\|_{\ell^1 \times \ell^1} \|H\|_{L^1} \\ &\leq \frac{\sqrt{\|\mathcal{T}_c G\|_{\ell^0 \times \ell^0} \|H\|_{L^0}}}{2\pi} \|\mathcal{T}_c G\|_{\ell^2 \times \ell^2} \|H\|_{L^2} \leq \frac{(2N+1) \sqrt{|\Omega|}}{2\pi} \|G\|_{\text{HS}} \|H\|_{\text{HS}}. \end{aligned}$$

□

In the following theorem $F_q^\delta|_{\Omega^c}$ denotes a noisy version of a restricted far field operator $F_q|_{\Omega^c}$ corresponding to a scatterer $D \subseteq B_R(c)$ that cannot be observed on $\Omega \subseteq S^1 \times S^1$. We assume that *a priori* information on the approximate location of the scatterer is available, i.e. that the ball $B_R(c)$ is known, and we establish a stability estimate for the least squares problem (4.1).

Theorem 4.2. *Suppose that $F_q, F_q^\delta \in \text{HS}(L^2(S^1))$, $c \in \mathbb{R}^2$, $N \in \mathbb{N}$, and $\Omega \subseteq S^1 \times S^1$ such that*

$$C := \frac{(2N+1) \sqrt{|\Omega|}}{2\pi} < 1.$$

Denote by \widetilde{F}_q and \widetilde{F}_q^δ the solutions to the least squares problems

$$F_q|_{\Omega^c} \stackrel{\text{LS}}{=} \widetilde{F}_q + \widetilde{B}_q, \quad \widetilde{F}_q \in \mathcal{V}_N^c, \widetilde{B}_q \in \mathcal{V}_\Omega, \quad (4.3a)$$

$$F_q^\delta|_{\Omega^c} \stackrel{\text{LS}}{=} \widetilde{F}_q^\delta + \widetilde{B}_q^\delta, \quad \widetilde{F}_q^\delta \in \mathcal{V}_N^c, \widetilde{B}_q^\delta \in \mathcal{V}_\Omega, \quad (4.3b)$$

respectively. Then,

$$\|\widetilde{F}_q^\delta - \widetilde{F}_q\|_{\text{HS}}^2 \leq (1 - C^2)^{-1} \|F_q^\delta|_{\Omega^c} - F_q|_{\Omega^c}\|_{\text{HS}}^2, \quad (4.4a)$$

$$\|\widetilde{B}_q^\delta - \widetilde{B}_q\|_{\text{HS}}^2 \leq (1 - C^2)^{-1} \|F_q^\delta|_{\Omega^c} - F_q|_{\Omega^c}\|_{\text{HS}}^2. \quad (4.4b)$$

Proof. Denoting $F := F_q|_{\Omega^c} - F_q^\delta|_{\Omega^c}$, $\tilde{F} := \tilde{F}_q - \tilde{F}_q^\delta \in \mathcal{V}_N^c$ and $\tilde{B} := \tilde{B}_q - \tilde{B}_q^\delta \in \mathcal{V}_\Omega$, the least squares property (4.3) implies that

$$\|F\|_{\text{HS}}^2 = \|\tilde{F} + \tilde{B}\|_{\text{HS}}^2 + \|F - (\tilde{F} + \tilde{B})\|_{\text{HS}}^2 \geq \|\tilde{F} + \tilde{B}\|_{\text{HS}}^2.$$

Therefore, using (4.2) and the arithmetic-geometric mean inequality yields

$$\begin{aligned} \|F\|_{\text{HS}}^2 &\geq \|\tilde{F}\|_{\text{HS}}^2 + \|\tilde{B}\|_{\text{HS}}^2 - 2|\langle \tilde{F}, \tilde{B} \rangle_{\text{HS}}| \geq \|\tilde{F}\|_{\text{HS}}^2 + \|\tilde{B}\|_{\text{HS}}^2 - 2C\|\tilde{F}\|_{\text{HS}}\|\tilde{B}\|_{\text{HS}} \\ &\geq \|\tilde{F}\|_{\text{HS}}^2 + \|\tilde{B}\|_{\text{HS}}^2 - C^2\|\tilde{F}\|_{\text{HS}}^2 - \|\tilde{B}\|_{\text{HS}}^2. \end{aligned} \quad (4.5)$$

This shows the first estimate in (4.4), and the second estimate is obtained by interchanging the roles of \tilde{F} and \tilde{B} in the last step of (4.5). \square

Remark 4.3. Similar to remark 3.11, including the reciprocity property (2.28) and replacing the space \mathcal{V}_N^c in theorem 4.2 by \mathcal{W}_N^c from (3.23) and (3.24) allows to improve the constant C in the stability estimate (4.4) by a factor of about $1/\sqrt{2}$. \diamond

Remark 4.4. As we already discussed in remark 3.12 for far field operator splitting, it would be possible to complete the far field operator F_q by completing the far field patterns $u_q^\infty(\cdot; d)$ for each illumination direction $d \in S^1$ individually using the methods developed in [29]. The stability estimate in [29, theorem 5.5] and in theorem 4.2 have the same structure, but again the constant C_N^Ω in theorem 4.2 is roughly the square of the corresponding constant in [29, theorem 5.5]. This means that one should use the data completion scheme developed in this work, when completing whole far field operators. \diamond

Several variants of this data completion scheme have been discussed for single far field patterns in [29], and these can in principle also be generalized to the setting considered in this work. For instance one can avoid the required *a priori* knowledge of the size $R > 0$ of the scatterer by reformulating the data completion problem as an $\ell^1 \times \ell^1$ minimization problem similar to theorem 3.18. Since the size of the support of the scatterer enters the stability estimate in theorem 4.2 via the parameter $N \gtrsim kR$, it is often advantageous to combine far field operator completion with far field operator splitting to obtain better stability properties. In theorem 4.5 below we provide a corresponding stability result. It can be shown by combining the proofs of the theorems 3.15 and 4.2, and the proof is therefore omitted.

Theorem 4.5. Suppose that $F_q, F_q^\delta \in \text{HS}(L^2(S^1))$, $c_1, c_2 \in \mathbb{R}^2$, $N_1, N_2 \in \mathbb{N}$, and $\Omega \subseteq S^1 \times S^1$. We define

$$C := \frac{(2N_1 + 1)(2N_2 + 1)}{(k|c_1 - c_2|)^{\frac{3}{2}}} \quad \text{and} \quad C_{j,l} := \frac{\sqrt{(2N_j + 1)(2N_l + 1)}\sqrt{|\Omega|}}{2\pi},$$

where $(j, l) \in \{1, 2\}^2$. We assume that, for all $(j, l) \in \{1, 2\}^2$,

$$\begin{aligned} M_{j,l} &:= \sqrt{C} \left(\sqrt{C} + (2N_j + 1) + (2N_l + 1) \right) + C_{j,l} < 1, \\ C_{1,2} + C_{1,2} + C_{2,1} + C_{2,2} &< 1. \end{aligned}$$

Denote by $\tilde{F}_{q_1}, \tilde{F}_{q_2}, \tilde{F}_{q_1, q_2}, \tilde{F}_{q_2, q_1}, \tilde{B}_q$ and $\tilde{F}_{q_1}^\delta, \tilde{F}_{q_2}^\delta, \tilde{F}_{q_1, q_2}^\delta, \tilde{F}_{q_2, q_1}^\delta, \tilde{B}_q^\delta$ the solutions to the least squares problems

$$F_q|_{\Omega^c} \stackrel{\text{LS}}{=} \tilde{F}_{q_1} + \tilde{F}_{q_2} + \tilde{F}_{q_1, q_2} + \tilde{F}_{q_2, q_1} + \tilde{B}_q, \quad \tilde{F}_{q_j} \in \mathcal{V}_{N_j}^{c_j}, \tilde{F}_{q_j, q_l} \in \mathcal{V}_{N_j, N_l}^{c_j, c_l}, \tilde{B}_q \in \mathcal{V}_\Omega, \quad (4.6a)$$

$$F_q^\delta|_{\Omega^c} \stackrel{\text{LS}}{=} \tilde{F}_{q_1}^\delta + \tilde{F}_{q_2}^\delta + \tilde{F}_{q_1, q_2}^\delta + \tilde{F}_{q_2, q_1}^\delta + \tilde{B}_q^\delta, \quad \tilde{F}_{q_j}^\delta \in \mathcal{V}_{N_j}^{c_j}, \tilde{F}_{q_j, q_l}^\delta \in \mathcal{V}_{N_j, N_l}^{c_j, c_l}, \tilde{B}_q^\delta \in \mathcal{V}_\Omega, \quad (4.6b)$$

respectively. Then,

$$\|\tilde{F}_{q_j} - \tilde{F}_{q_j}^\delta\|_{\text{HS}}^2 \leq (1 - (M_{j,j} + C_{j,j}))^{-1} \|F_q - F_q^\delta\|_{\text{HS}}^2, \quad j = 1, 2, \quad (4.7a)$$

$$\|\tilde{B}_q - \tilde{B}_q^\delta\|_{\text{HS}}^2 \leq (1 - (C_{1,1} + C_{1,2} + C_{2,1} + C_{2,2}))^{-1} \|F_q - F_q^\delta\|_{\text{HS}}^2. \quad (4.7b)$$

5. Numerical examples

We briefly comment on the numerical implementation and illustrate the performance of our far field operator splitting and completion methods. As before, let $D = D_1 \cup D_2$ be a scatterer with two well-separated components $D_j \subseteq B_{R_j}(c_j)$ for some $c_j \in \mathbb{R}^2$ and $R_j > 0, j = 1, 2$. Assuming that far field patterns cannot be observed on a subdomain $\Omega \subseteq S^1 \times S^1$ satisfying $\Omega^c = \Omega^{c,r}$, i.e. given the noisy restricted far field operator $G := F_q^\delta|_{\Omega^c}$ we aim to recover the non-observable part $B := F_q|_{\Omega^c} - F_q$ and the far field operator components F_{q_1} and F_{q_2} associated to the two scatterer components individually.

The least squares approach from theorem 4.5 requires to solve

$$G \stackrel{\text{LS}}{=} \tilde{F}_{q_1} + \tilde{F}_{q_2} + \tilde{F}_{q_1, q_2} + \tilde{F}_{q_2, q_1} + \tilde{B}, \quad (5.1)$$

$$\tilde{F}_{q_1} \in \mathcal{V}_{N_1}^{c_1}, \tilde{F}_{q_2} \in \mathcal{V}_{N_2}^{c_2}, \tilde{F}_{q_1, q_2} \in \mathcal{V}_{N_1, N_2}^{c_1, c_2}, \tilde{F}_{q_2, q_1} \in \mathcal{V}_{N_2, N_1}^{c_2, c_1}, \tilde{B} \in \mathcal{V}_\Omega.$$

If the assumptions of theorem 4.5 are fulfilled, then the solution to (5.1) can be approximated efficiently using conjugate gradients. On the other hand, the $\ell^1 \times \ell^1$ approach in theorem 3.18 can also be extended to simultaneously splitting and completing far field operators. Introducing a Lagrange multiplier $1/\mu > 0$ the associated unconstrained optimization problem consists in minimizing

$$\Psi_\mu(F_{q_1}, F_{q_2}, F_{q_1, q_2}, F_{q_2, q_1}) := \left\| G - \mathcal{P}_\Omega(F_{q_1} + F_{q_2} + F_{q_1, q_2} + F_{q_2, q_1}) \right\|_{\text{HS}}^2 \quad (5.2)$$

$$+ \mu (\| \mathcal{T}_{c_1} F_{q_1} \|_{\ell^1 \times \ell^1} + \| \mathcal{T}_{c_2} F_{q_2} \|_{\ell^1 \times \ell^1} + \| \mathcal{T}_{c_1, c_2} F_{q_1, q_2} \|_{\ell^1 \times \ell^1} + \| \mathcal{T}_{c_2, c_1} F_{q_2, q_1} \|_{\ell^1 \times \ell^1})$$

with respect to $(F_{q_1}, F_{q_2}, F_{q_1, q_2}, F_{q_2, q_1}) \in \text{HS}(L^2(S^1))^4$. The unique minimizer $(\tilde{F}_{q_1}, \tilde{F}_{q_2}, \tilde{F}_{q_1, q_2}, \tilde{F}_{q_2, q_1})$ of Ψ_μ can be approximated using iterative soft thresholding (see [4, 16]). Then $\tilde{F}_q := \tilde{F}_{q_1} + \tilde{F}_{q_2} + \tilde{F}_{q_1, q_2} + \tilde{F}_{q_2, q_1}$ is an approximation to F_q , and $\tilde{B} := -\mathcal{P}_\Omega \tilde{F}_q$ approximates the non-observable part B .

We discuss three examples, where we use $k = 0.5$ and $q = -0.5\chi_{D_1} + \chi_{D_2}$. Example 5.1 is concerned with far field operator splitting only, i.e. $\Omega = \emptyset$, while in example 5.2 we consider far field operator completion but without splitting, i.e. we view D as a single object. Finally, in example 5.3 we combine far field operator completion with far field operator splitting and show that this often yields better results.

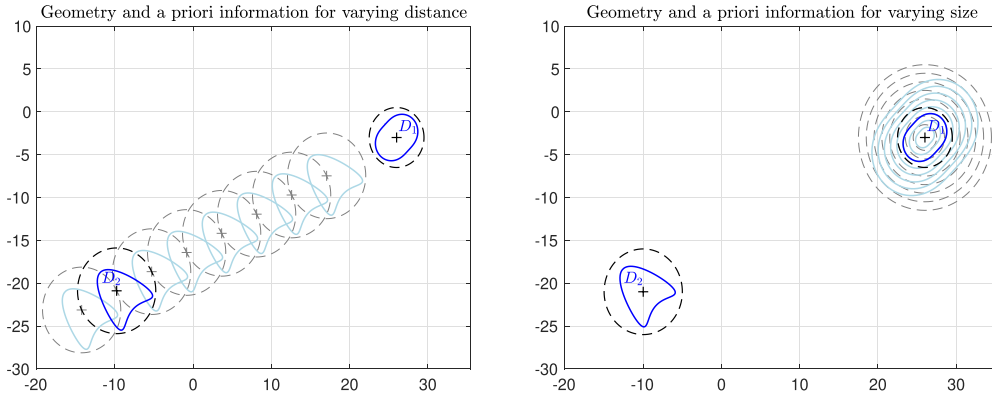


Figure 4. Left: geometry of scatterer (solid) and *a priori* information on location and size of components (dashed) in example 5.1 for varying distance ($|c_1 - c_2| = 40$ highlighted). Right: geometry of scatterer (solid) and *a priori* information on location and size of components (dashed) in example 5.1 for varying size of D_1 and varying R_1 ($R_1 = 3.5$ highlighted).

Example 5.1. We study the accuracy of the numerical reconstructions for far field operator splitting depending on the distance between the two components of the scatterer, and with respect to the size of these components. In our first test, we vary $|c_1 - c_2|$ as depicted in figure 4(left), using $R_1 = 3.5$ and $R_2 = 5$, and in our second test, we vary the size of D_1 and R_1 as shown in figure 4(right). We apply a Nyström method to evaluate the far field operator F_q for $L = 256$ equidistant illumination and observation directions on S^1 for each of these configurations. We add 5% complex valued uniformly distributed additive relative error to F_q and denote the result by F_q^δ .

To solve the far field operator splitting problem using the least squares approach, we assume the dashed circles in figure 4 to be known *a priori*. Accordingly, we choose $N_1 = 3$ and $N_2 = 7$ for the first test, and $N_1 \in \{2, 2, 3, 4, 4, 5, 6, 6\}$ and $N_2 = 4$ for the second test. For the $l^1 \times l^1$ approach, we use $\mu = 10^{-3}$ in (5.2). In contrast to the least squares method no *a priori* information on the approximate size of the components D_1 and D_2 but only the approximate positions c_1 and c_2 are required. These are indicated by the two crosses inside D_1 and D_2 in figure 4. We also simulate the far field operators $F_{q_j}, j = 1, 2$, corresponding to the two scatterers individually using the Nyström method and compare them to the results of our reconstruction method by evaluating relative reconstruction errors

$$\epsilon_{\text{rel}}^j := \frac{\|F_{q_j} - \tilde{F}_{q_j}\|_{\text{HS}}}{\|F_{q_j}\|_{\text{HS}}}, \quad j = 1, 2.$$

In figure 5 these relative errors are shown. The left plot corresponds to our first test with varying distance between the two components of the scatterers, and the right plot corresponds to our second test with varying diameter of the first component. By and large, the relative errors decay with increasing distance and also with decreasing diameter. This is to be expected because the accuracy of the second order Born approximation and also the stability of both reconstruction algorithms improve in this case (see theorems 3.15 and 3.18). Both computational approaches yield satisfying results of comparable accuracy. \diamond

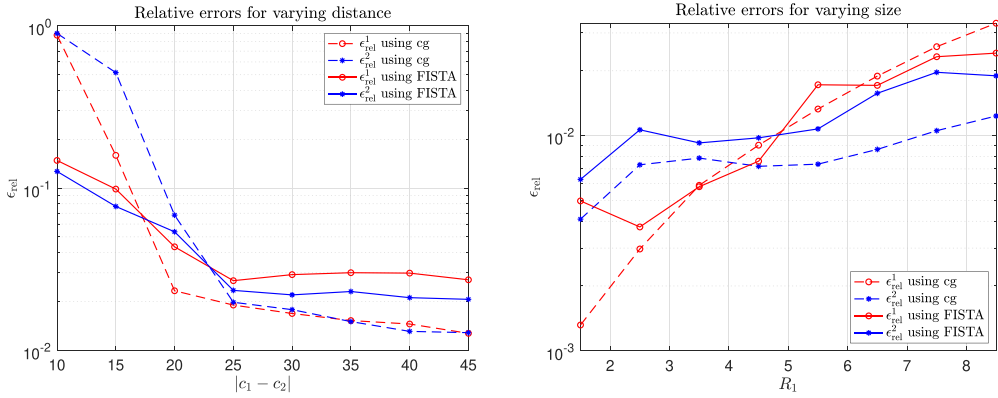


Figure 5. Left: relative errors of far field operator splitting for varying distance $|c_1 - c_2|$. Right: relative errors of far field operator splitting for varying size of scatterer D_1 .

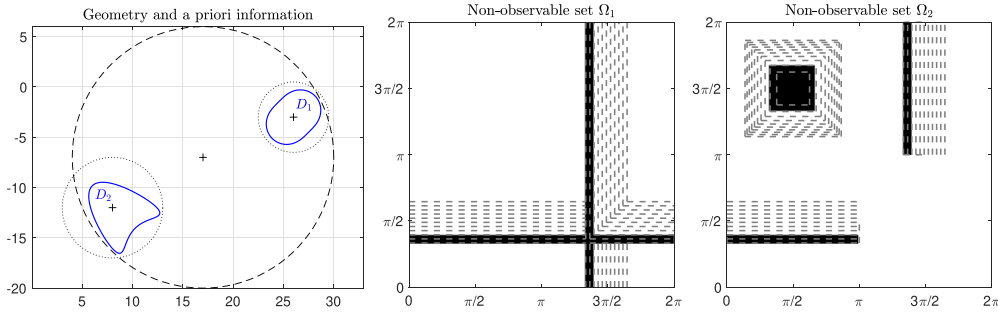


Figure 6. Left: geometry of scatterer (solid), *a priori* information on location of scatterer (dashed) in example 5.2, and *a priori* information on location of components of scatterer (dotted) in example 5.3. Center: support of missing data segment $\Omega_1(\alpha)$ for varying width α ($\Omega_1(\pi/16)$ highlighted). Right: support of missing data segment $\Omega_2(\alpha)$ for varying width α ($\Omega_2(\pi/16)$ highlighted).

Example 5.2. We consider far field operator completion and study the accuracy of numerical reconstructions depending on the size $|\Omega|$ of the non-observable part Ω . The geometry of the scatterer $D = D_1 \cup D_2$ is shown in figure 6(left). In our first test, we assume that the missing data segment $\Omega_1(\alpha)$ is supported on a union of two strips of width $\alpha \in \{\frac{\pi}{32}, \frac{2\pi}{32}, \dots, \frac{10\pi}{32}\}$, as shown (in polar coordinates) in figure 6(center). In our second test, we suppose that the missing data segment $\Omega_2(\alpha)$ is supported on a union of two strips of width α and a square with side length $\beta := \sqrt{\alpha(2\pi - \alpha)}$ for $\alpha \in \{\frac{\pi}{32}, \frac{2\pi}{32}, \dots, \frac{10\pi}{32}\}$, as shown in figure 6(right). Accordingly, the relative area of the missing data segments is given by

$$\frac{|\Omega_1(\alpha)|}{4\pi^2} = \frac{|\Omega_2(\alpha)|}{4\pi^2} \in \{3\%, 6\%, \dots, 31\%\}.$$

We simulate the associated far field operators using a Nyström method with $L=256$ equidistant illumination and observation directions on S^1 , and we add 5% complex valued uniformly distributed additive relative error.

To solve the far field operator completion problem using the least squares approach, we assume the dashed circle in figure 6 to be known *a priori*. Accordingly, we choose $N=9$. For

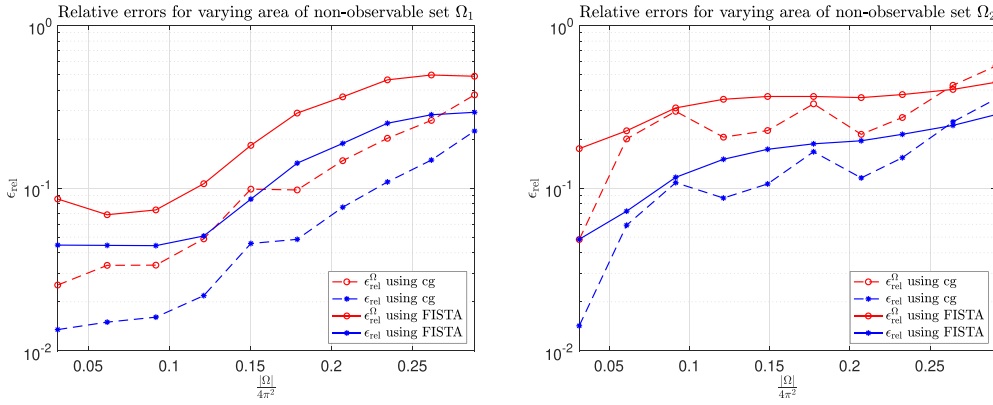


Figure 7. Relative errors of far field operator completion. Left: cross-shaped missing data segment $\Omega = \Omega_1$. Right: disconnected missing data segment $\Omega = \Omega_2$.

the $\ell^1 \times \ell^1$ approach (without splitting) we use $\mu = 10^{-3}$. We evaluate relative errors

$$\epsilon_{\text{rel}} := \frac{\|F_q - \tilde{F}_q\|_{\text{HS}}}{\|F_q\|_{\text{HS}}} \quad \text{and} \quad \epsilon_{\text{rel}}^{\Omega} := \frac{\|B - \tilde{B}\|_{\text{HS}}}{\|B\|_{\text{HS}}}$$

for the reconstructed far field operator \tilde{F}_q and for the reconstructed non-observable part \tilde{B} . The results are shown in figure 7. The left and right plot correspond to our first and second test with the missing data segment $\Omega = \Omega_1$ and $\Omega = \Omega_2$, respectively. By and large, the relative reconstruction errors mostly decays with decaying area of Ω in both cases. The least squares approach yields slightly better reconstructions than the $\ell^1 \times \ell^1$ approach. The two examples show that the quality of the reconstruction not only depends on the area $|\Omega|$ of the missing data segment but also on the geometric structure of Ω . \diamond

Example 5.3. We consider the same setting as in example 5.2 but now we combine far field operator splitting and completion and show that this leads to better numerical reconstructions than those of example 5.2. For the least squares approach we assume the dotted circles in figure 6(left) to be known *a priori*. Accordingly, we use $N_1 = 3$ and $N_2 = 4$ in (5.1). For the associated $\ell^1 \times \ell^1$ minimization problem (5.2) we use $\mu = 10^{-3}$. Again the data contain 5% complex valued uniformly distributed additive relative error. We evaluate relative errors

$$\epsilon_{\text{rel}} := \frac{\|F_q - \tilde{F}_{q_1} - \tilde{F}_{q_2} - \tilde{F}_{q_1, q_2} - \tilde{F}_{q_2, q_1}\|_{\text{HS}}}{\|F_q\|_{\text{HS}}} \quad \text{and} \quad \epsilon_{\text{rel}}^{\Omega} := \frac{\|B - \tilde{B}\|_{\text{HS}}}{\|B\|_{\text{HS}}}$$

for the reconstructed far field operator \tilde{F}_q and for the reconstructed non-observable part \tilde{B} . The results are shown in figure 8. The left plot corresponds to our first test with the missing data segment $\Omega = \Omega_1$, and the right plot corresponds to our second test with $\Omega = \Omega_2$. When comparing figures 7 and 8, we find that combining far field operator completion with far field operator splitting yields more accurate results. This is due to the fact that $N_1 + N_2 = 7 < 9 = N$, where N denotes the parameter determining the dimension of the space \mathcal{V}_N^c in example 5.2. Accordingly, sparser representations are used when combining far field operator completion with far field operator splitting, which leads to increased stability (see also theorem 4.5). \diamond

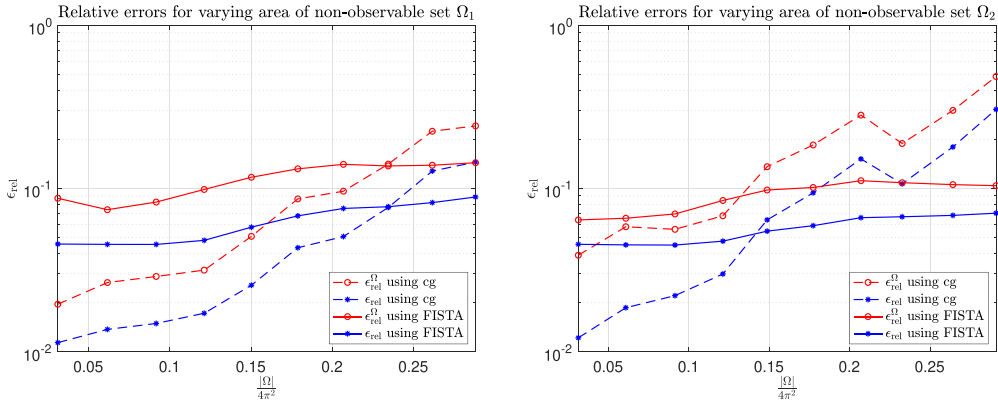


Figure 8. Relative errors of simultaneous far field operator completion and splitting. Left: cross-shaped missing data segment $\Omega = \Omega_1$. Right: disconnected missing data segment $\Omega = \Omega_2$.

6. Conclusions

Untangling multiple scattering effects to approximate the scattering response of each scatterer in an ensemble of several scattering objects from scattering data for the whole ensemble is a basic question in inverse scattering theory. We have developed conditions on how far apart two scatterers have to be in order to be able to split their far field operator with a reasonable condition number. Closely related is the question of resolution in inverse scattering, i.e. how far apart do two scatterers have to be in order to be able to distinguish them in a reconstruction.

We have also discussed the data completion problem to recover missing or corrupted scattering data segments in remote observations. We have established conditions on how large the area covered by the affected illumination or observation directions in the scattering data can be in order to guarantee that the associated far field operator can be reconstructed with a reasonable condition number.

For both inverse problems we have seen that these conditions for well-posedness are less restrictive for scattering problems and associated far field operators than for source problems and associated single far field patterns as considered in [29]. In fact, the correlation between scattered waves corresponding to different incident plane waves improves the stability.

Data availability statement

The data that support the findings of this study are openly available at the following URL/DOI: <https://gitlab.kit.edu/kit/ianm/ag-ip/software/2024-rg-ls-ff-op-splitting>.

Acknowledgments

The first author would like to thank John Sylvester for helpful conversations on the topic of this work. The research for this paper was supported by Deutsche Forschungsgemeinschaft (DFG, German Research Foundation)—Project-ID 258734477—SFB 1173.

ORCID iDs

Roland Griesmaier  <https://orcid.org/0000-0002-1621-6127>

Lisa Schätzle  <https://orcid.org/0009-0004-8320-8014>

References

- [1] Audibert L and Haddar H 2014 A generalized formulation of the linear sampling method with exact characterization of targets in terms of farfield measurements *Inverse Problems* **30** 035011
- [2] Aussal M, Boukari Y and Haddar H 2020 Data completion method for the Helmholtz equation via surface potentials for partial Cauchy data *Inverse Problems* **36** 055012
- [3] Baffet D and Grote M J 2019 On wave splitting, source separation and echo removal with absorbing boundary conditions *J. Comput. Phys.* **387** 589–96
- [4] Beck A and Teboulle M 2009 A fast iterative shrinkage-thresholding algorithm for linear inverse problems *SIAM J. Imaging Sci.* **2** 183–202
- [5] ben Hassen F, Liu J and Potthast R 2007 On source analysis by wave splitting with applications in inverse scattering of multiple obstacles *J. Comput. Math.* **25** 266–81
- [6] Borcea L, Druskin V, Mamonov A V and Zaslavsky M 2018 Untangling the nonlinearity in inverse scattering with data-driven reduced order models *Inverse Problems* **34** 065008
- [7] Boukari Y and Haddar H 2015 A convergent data completion algorithm using surface integral equations *Inverse Problems* **31** 035011
- [8] Bukhgeim A L 2008 Recovering a potential from Cauchy data in the two-dimensional case *J. Inverse Ill-Posed Problems* **16** 19–33
- [9] Cakoni F and Colton D 2014 *A Qualitative Approach to Inverse Scattering Theory (Applied Mathematical Sciences vol 188)* (Springer)
- [10] Cakoni F, Colton D and Haddar H 2023 *Inverse Scattering Theory and Transmission Eigenvalues (CBMS-NSF Regional Conf. Series in Applied Mathematics vol 98)* 2nd edn (Society for Industrial and Applied Mathematics (SIAM))
- [11] Cogar S, Colton D, Meng S and Monk P 2017 Modified transmission eigenvalues in inverse scattering theory *Inverse Problems* **33** 125002
- [12] Colton D and Kirsch A 1996 A simple method for solving inverse scattering problems in the resonance region *Inverse Problems* **12** 383–93
- [13] Colton D and Kress R 1995 Eigenvalues of the far field operator for the Helmholtz equation in an absorbing medium *SIAM J. Appl. Math.* **55** 1724–35
- [14] Colton D and Kress R 2019 *Inverse Acoustic and Electromagnetic Scattering Theory (Applied Mathematical Sciences vol 93)* 4th edn (Springer)
- [15] Colton D and Monk P 1988 The inverse scattering problem for time-harmonic acoustic waves in an inhomogeneous medium *Q. J. Mech. Appl. Math.* **41** 97–125
- [16] Daubechies I, Defrise M and De Mol C 2004 An iterative thresholding algorithm for linear inverse problems with a sparsity constraint *Commun. Pure Appl. Math.* **57** 1413–57
- [17] DeFilippis N, Moskow S and Schotland J C 2023 Born and inverse Born series for scattering problems with Kerr nonlinearities *Inverse Problems* **39** 125015
- [18] Olver F W J, Olde Daalhuis A B, Lozier D W, Schneider B I, Boisvert R F, Clark C W, Miller B R, Saunders B V, Cohl H S and McClain M A (eds) NIST digital library of mathematical functions, Release 1.1.11 of 15 September 2023 (available at: <https://dlmf.nist.gov/>)
- [19] Donoho D L and Stark P B 1989 Uncertainty principles and signal recovery *SIAM J. Appl. Math.* **49** 906–31
- [20] Dou F, Liu X, Meng S and Zhang B 2022 Data completion algorithms and their applications in inverse acoustic scattering with limited-aperture backscattering data *J. Comput. Phys.* **469** 111550
- [21] Druskin V, Mamonov A V, Thaler A E and Zaslavsky M 2016 Direct, nonlinear inversion algorithm for hyperbolic problems via projection-based model reduction *SIAM J. Imaging Sci.* **9** 684–747
- [22] Druskin V, Mamonov A V and Zaslavsky M 2018 A nonlinear method for imaging with acoustic waves via reduced order model backprojection *SIAM J. Imaging Sci.* **11** 164–96

- [23] Engquist B and Zhao H 2018 Approximate separability of the Green's function of the Helmholtz equation in the high-frequency limit *Commun. Pure Appl. Math.* **71** 2220–74
- [24] Graff M, Grote M J, Nataf F and Assous F 2019 How to solve inverse scattering problems without knowing the source term: a three-step strategy *Inverse Problems* **35** 104001
- [25] Griesmaier R, Hanke M and Sylvester J 2014 Far field splitting for the Helmholtz equation *SIAM J. Numer. Anal.* **52** 343–62
- [26] Griesmaier R and Harrach B 2018 Monotonicity in inverse medium scattering on unbounded domains *SIAM J. Appl. Math.* **78** 2533–57
- [27] Griesmaier R, Hyvönen N and Seiskari O 2013 A note on analyticity properties of far field patterns *Inverse Problems Imaging* **7** 491–8
- [28] Griesmaier R and Sylvester J 2016 Far field splitting by iteratively reweighted ℓ^1 minimization *SIAM J. Appl. Math.* **76** 705–30
- [29] Griesmaier R and Sylvester J 2017 Uncertainty principles for inverse source problems, far field splitting and data completion *SIAM J. Appl. Math.* **77** 154–80
- [30] Griesmaier R and Sylvester J 2017 Uncertainty principles for three-dimensional inverse source problems *SIAM J. Appl. Math.* **77** 2066–92
- [31] Griesmaier R and Sylvester J 2018 Uncertainty principles for inverse source problems for electromagnetic and elastic waves *Inverse Problems* **34** 065003
- [32] Grote M J, Kray M, Nataf F and Assous F 2017 Time-dependent wave splitting and source separation *J. Comput. Phys.* **330** 981–96
- [33] Kilgore K, Moskow S and Schotland J C 2012 Inverse Born series for scalar waves *J. Comput. Math.* **30** 601–14
- [34] Kilgore K, Moskow S and Schotland J C 2017 Convergence of the Born and inverse Born series for electromagnetic scattering *Appl. Anal.* **96** 1737–48
- [35] Kirsch A 1998 Characterization of the shape of a scattering obstacle using the spectral data of the far field operator *Inverse Problems* **14** 1489–512
- [36] Kirsch A 2017 Remarks on the Born approximation and the factorization method *Appl. Anal.* **96** 70–84
- [37] Kirsch A 2021 *An Introduction to the Mathematical Theory of Inverse Problems (Applied Mathematical Sciences vol 120)* 3rd edn (Springer)
- [38] Kirsch A and Grinberg N 2008 *The Factorization Method for Inverse Problems (Oxford Lecture Series in Mathematics and its Applications vol 36)* (Oxford University Press)
- [39] Krasikov I 2006 Uniform bounds for Bessel functions *J. Appl. Anal.* **12** 83–91
- [40] Landau L J 2000 Bessel functions: monotonicity and bounds *J. London Math. Soc.* **61** 197–215
- [41] Liu X and Sun J 2019 Data recovery in inverse scattering: from limited-aperture to full-aperture *J. Comput. Phys.* **386** 350–64
- [42] Nachman A I 1988 Reconstructions from boundary measurements *Ann. Math.* **128** 531–76
- [43] Natterer F 2004 An error bound for the Born approximation *Inverse Problems* **20** 447–52
- [44] Novikov R G 1988 A multidimensional inverse spectral problem for the equation $-\Delta\psi + (v(x) - Eu(x))\psi = 0$ *Funktsional. Anal. i Prilozhen.* **22** 11–22, 96
- [45] Potthast R, Fazi F M and Nelson P A 2010 Source splitting via the point source method *Inverse Problems* **26** 045002
- [46] Ramm A G 1988 Recovery of the potential from fixed-energy scattering data *Inverse Problems* **4** 877–86
- [47] Reed M and Simon B 1972 *Methods of Modern Mathematical Physics. I. Functional Analysis* (Academic)
- [48] Saranen J and Vainikko G 2002 *Periodic Integral and Pseudodifferential Equations With Numerical Approximation* (Springer Monographs in Mathematics) (Springer)
- [49] Sylvester J 2009 An estimate for the free Helmholtz equation that scales *Inverse Problems Imaging* **3** 333–51
- [50] Vainikko G 2000 Fast solvers of the Lippmann-Schwinger equation *Direct and Inverse Problems of Mathematical Physics (Newark, DE, 1997) (International Society for Analysis, Applications and Computation vol 5)* (Kluwer Academic Publishers) pp 423–40